https://doi.org/10.5194/egusphere-2023-2949
Preprint. Discussion started: 15 January 2024

Seasonal, regional and vertical characteristics of high carbon monoxide plumes along with their associated ozone anomalies as seen by IAGOS between 2002 and 2019

Thibaut Lebourgeois[1,2], Bastien Sauvage[1], Pawel Wolff[3], Béatrice Josse[2], Virginie Marécal[2], Yasmine Bennouna[1], Romain Blot[1], Damien Boulanger[3], Hannah Clark[1], Jean-Marc Cousin[1], Philippe Nedelec[1], and Valérie Thouret[1]

[1]Laboratoire d'Aérologie, Université de Toulouse, CNRS, UPS, Toulouse, France
[2]CNRM, Université de Toulouse, Météo-France, CNRS, Toulouse, France
[3]Observatoire Midi-Pyrénées, Université de Toulouse, CNRS, UPS, 31400 Toulouse, France

Correspondence: Thibaut Lebourgeois (thibaut.lebourgeois@aero.obs-mip.fr)

https://doi.org/10.5194/egusphere-2023-2949
Preprint. Discussion started: 15 January 2024

In-situ measurements from IAGOS are used to characterise extreme values of carbon monoxide (CO) in the troposphere between 2002 and 2019. The SOFT-IO model, combining the FLEXPART lagrangian dispersion model with emission inventories over the footprint region is used to identify the origins of the CO in the sampled plumes. The impact of biomass burning and anthropogenic emissions on such CO plumes are characterised through CO mixing ratios and simultaneously recorded ozone (O_3) ones.

In the Northern Hemisphere, maximum of CO are reached in DJF in the lower troposphere because of the elevated anthropogenic emissions and reduced convective activity of the season. Due to the low photochemistry and the fresh age of the air mass the O_3 values of these plumes are low. CO plumes in the upper troposphere result from intense emissions and efficient vertical transport, peaking during JJA. Among the anomalies detected in the UT in JJA, the ones with the higher associated O_3 values are the ones associated with biomass burning emissions. The middle troposphere combines the two previous vertical levels with contributions from both local emissions and long-range transport. The emission regimes and meteorological conditions are fundamentally different within the troposphere over Africa. Convection is no longer the limiting factor and the transport of the CO plumes is driven by the ITCZ shift, trade winds and the upper branch of the Hadley cell redistributing the pollution to higher latitudes.

https://doi.org/10.5194/egusphere-2023-2949
Preprint. Discussion started: 15 January 2024

1 Introduction

Extreme weather and climate events are still known for being incorrectly reproduced and predicted by the global and regional models. Extreme pollution events suffer the same weaknesses, because they can be explained by multiple factors such as abnormal weather conditions and/or unusually intense emissions (either from anthropogenic or natural sources, or both). Hence, it is essential to better understand the distributions of some pollutants or their precursors in the atmosphere under such circumstances, leading thus to a better representation by the models and an improvement of their ability to predict their peak values as well as their impact on climate. Among the short-lived climate forcers, tropospheric ozone (O_3) is a key compound of our atmosphere, and carbon monoxide (CO) is one of its main precursors. First, O_3 is a pollutant dangerous for human life (Chen et al., 2007; Liu et al., 2018) and for crops (Fuhrer et al., 1997; Davison and Barnes, 1998; Ashmore, 2005). Secondly, it is a trace gas with major influence on the oxidative capacity of the atmosphere as it is the main source of hydroxyl radicals in the troposphere (Seinfeld and Pandis, 2008). Finally, it is a greenhouse gas (GHG) with a positive radiative effect in the troposphere, moreover multiple studies have shown the upper troposphere lower stratosphere (UTLS) to be the region with the largest changes in radiative effect from its changes in O_3 mixing ratio (Riese et al., 2012; Xia et al., 2018).

O_3 can hence have an impact on air quality as much as on climate. This compound is photochemically produced from NOx and VOC (Volatile Organic Compounds)/CO (Seinfeld and Pandis, 2008). Hence, a good estimation of its chemical precursors as well as better understanding of the process leading their distributions at global scale is of prime importance.

For these reasons, this study is focused on the most intense anomalies of CO throughout the troposphere over different regions of the world and how O_3 distributions behave in such plumes.

Apart from being a precursor of O_3, CO is also one of the biggest sinks of hydroxyl radical (Lelieveld et al., 2016) and thus has an impact on the oxidative capacity of the atmosphere which can lead to increase the lifetime of other greenhouse gases such as CH_4. Moreover, the oxidation of CO produces greenhouse gases like O_3 and CO_2. CO is hence believed to cause an indirect positive radiative forcing (IPCC, 2013). Finally, CO is a good tracer for pollution export pathways thanks to its long chemical lifetime in the troposphere of a few weeks in summer to a few months in winter (Lelieveld et al., 2016).

CO is mostly emitted in the planetary boundary layer (BL) and can be removed via different mechanisms. These mechanisms highly depend on the regions and seasons. Convective activity represents an important part of the pollution export pathways from the BL. Some regions are more prone than others to exporting pollutants. Tropical regions benefit from permanent convective activity due to the close proximity of the Inter-Tropical Convergence Zone (ITCZ) (Andreae et al., 2001; Lannuque et al., 2021). Regions like south and eastern Asia benefit from the different phases of the monsoon season or cold front and warm conveyor belt activity (Ricaud et al., 2014; Park et al., 2007; Lawrence, 2004; Liang et al., 2004). North American pollution is mostly exported through cold front and warm conveyor belt (Owen et al., 2006). CO from biomass burning in boreal regions can be emitted directly above the BL and as high as the upper troposphere (UT) through pyroconvection whereas tropical fires emit mainly in the BL (Rémy et al., 2017; Val Martin et al., 2010; Damoah et al., 2006). Once in the free troposphere, CO is transported via westerlies or jet streams. For example, it is not rare to find CO-rich air masses in North America which originated in Eastern Asia (Liang et al., 2004). In special cases, heavily polluted air masses can reach the UT (e.g. Nedelec

https://doi.org/10.5194/egusphere-2023-2949
Preprint. Discussion started: 15 January 2024

et al. (2005)). Those events happen when polluted air masses are transported upward by strong convective episodes and can have a relatively large impact on the chemistry in the UT.

Among O_3 precursors only CO has a chemical lifetime long enough to reach the UT, so in this part of the atmosphere CO is hence believed to have an impact on O_3 mixing ratio as long as reservoirs for NOx are available.

Moreover, large values of CO in the UT are an indication of surface influenced air masses potentially rich in many pollutants emitted at the surface, which illustrates the importance of better understanding phenomena able to bring vast amounts of CO in the upper part of the troposphere.

Studies on the export of large quantities of CO in the free troposphere or above have been facilitated with the access to satellite data. An important number of studies have been focused on the eastern/southern part of Asia and especially on the export of the CO emitted into different regions (e.g. Fadnavis et al. (2011); Barret et al. (2016); Smoydzin and Hoor (2022)). Barret et al. (2016) used data from IASI onboard MetOp-A satellite in order to analyse the provenance of the pollution in the upper tropospheric South Asian Monsoon Anticyclone (SAMA) and showed that emissions from the Indo-Gangetic plain were uplifted during the Asian summer monsoon and trapped in its upper level anticyclone. Smoydzin and Hoor (2022) recently used MOPITT to investigate large CO anomalies in the North Pacific and attributed those extremes to emissions from East Asia. Lannuque et al. (2021) used the IAGOS dataset to characterise the seasonal variability of CO in the African upper troposphere, which is mostly regionally emitted. The variations in its seasonal cycle are correlated with the shift of the Inter-Tropical Convergence Zone (ITCZ).

Huang et al. (2012) showed that the most extreme events of CO in this part of the atmosphere were caused by vertical transport close to the region of emissions by different processes like cold fronts or tropical cyclones.

This emphasises the importance of transport when studying CO extremes in remote parts of the atmosphere. Most of the studies cited above focused on the export of plumes of high CO mixing ratios in one region at a certain altitude and only a few of them were focused on the most extreme CO anomalies. Thanks to the IAGOS Research Infrastructure (In-service Aircraft for a Global Observing System; http://www.iagos.org), we benefit from a large, and long-term in-situ sampling of the atmosphere, complementing the dedicated field campaigns and more global satellite datasets. We present here a quasi-global overview over almost 20 years of extreme CO mixing ratios and their associated O_3 values, as seen by IAGOS.

The goal of this paper is to characterise the seasonal, regional and vertical CO mixing ratios anomalies for different regions over the globe for almost 20 years as seen by IAGOS along with the simultaneously recorded O_3 between 2002 and 2019. The analysis will explore CO anomalies and their source type (anthropogenic vs biomass burning) and region of emission (14 defined regions of the Global Fire Emissions Database (GFED) (Giglio et al., 2013)). It aims at characterising the distributions and origins of extreme events of polluted plumes in terms of (i) mixing ratios of CO and O3, (ii) frequency and seasonality at different altitudes. Such characteristics will form a set of diagnostics that are of particular importance to further test the ability of the models to reproduce extreme events and their impact on the distributions of CO and O_3 throughout the troposphere.

https://doi.org/10.5194/egusphere-2023-2949
Preprint. Discussion started: 15 January 2024

2 Methods and materials

2.1 IAGOS dataset

The data used in this study is from the European research infrastructure IAGOS (Petzold et al., 2015; Thouret et al., 2022)), which has measured different trace gases, particles and meteorological components from passenger airplanes over several decades. IAGOS builds on the experience of the MOZAIC programme (Marenco et al., 1998), which was originally set up in 1994. O_3 and water vapour were the initial compounds measured, with CO measurements added in December 2001. O_3 and CO are measured with an UV and infrared absorption photometer respectively (Thouret et al., 1998; Nédélec et al., 2015), with a total uncertainty of $\pm$ 2 ppb $\pm$ 2% for O_3 and $\pm$ 5 ppb $\pm$ 5% for CO with a time resolution of 4 seconds and 30 seconds respectively. IAGOS took over from MOZAIC in 2011, including an overlap period between 2011 and 2014 (Petetin et al., 2016). The IAGOS European Research Infrastructure also includes the predecessor complementary program CARIBIC (Brenninkmeijer et al., 1999). The consistency between the MOZAIC, IAGOS and CARIBIC datasets have been tested and they are considered as a unique dataset (Blot et al., 2021).

As this study focuses on CO and O_3, the dataset used is from the start of the CO measurement (January 2002) to December 2019. This dense network of measurements allows an unprecedented number of pollution events to be sampled for an in-situ dataset with a higher vertical resolution than satellite datasets. In total, more than 43 000 flights were performed by the different aircraft during this period. These flights were performed by 10 different airlines allowing the in situ measurements in several regions of the world. In addition, each flight takes two vertical profiles (during take-off and landing). In contrast with other in-situ datasets from field campaigns, IAGOS is not dedicated to the study of a single phenomenon but rather to the long-term sampling of the atmosphere. This makes the large and precise IAGOS data set particularly suitable for a thorough analysis of the variability of the CO anomalies (see section 2.3.2 for the formal definition) in the different parts of the troposphere.

The model SOFT-IO (Sauvage et al., 2017) is used to attribute a source type (from biomass burning or anthropogenic emissions) and a geographical origin to all of our detected extreme mixing ratios of CO. This model is based on the Lagrangian particle dispersion model FLEXPART (Stohl et al., 2005) and emission inventories to compute the recent contribution from CO emissions to each IAGOS measurements. SOFT-IO has already been used several times to analyse the origins of such tropospheric CO plumes (e.g Tsivlidou et al. (2022); Petetin et al. (2018a); Cussac et al. (2020); Lannuque et al. (2021)).

2.2 SOFT-IO, The source-receptor link

Since IAGOS is not a research project focused on the study of one phenomenon of the atmosphere but a global exploratory observing system sampling the atmosphere regardless of its current state, a tool was needed to get information on the type of source influencing the air mass (biomass burning or anthropogenic emissions). This is the main usage of the SOFT-IO model.

SOFT-IO is described in detail in Sauvage et al. (2017) and used in scientific studies (e.g. Petetin et al. (2018b); Lannuque et al. (2021); Cussac et al. (2020); Tsivlidou et al. (2022)) so only a broad description of the model is given here. SOFT-IO is a model based on FLEXPART (Stohl et al., 2005) and emission inventories of anthropogenic and biomass burning sources (described below) along the IAGOS flight tracks. A 20-day back trajectory is coupled to the emission inventories to calculate

https://doi.org/10.5194/egusphere-2023-2949
Preprint. Discussion started: 15 January 2024

the CO contributions from recent emissions. The model uses wind fields from ERA interim with a horizontal resolution of $1° \times 1°$ and 137 vertical levels.

The Biomass Burning inventories used in this version of SOFT-IO is the 1.2 version of the Global Fire Assimilation System (GFAS) (Kaiser et al., 2012). The horizontal resolution is $0.1° \times 0.1°$ with a daily temporal resolution. The emission top altitude is provided by GFAS (v1.2), and is calculated using the wildfire plume rise model from (Paugam et al., 2015). GFAS was chosen for its temporal resolution as well as its ability to model emission height. The anthropogenic emissions are from the Community Emissions Data System (CEDS2) (McDuffie et al., 2020) with a resolution of $0.5° \times 0.5°$ and a monthly temporal resolution.

SOFT-IO models the CO source contributions and the geographical origin of the emitted CO. The geographical origin of the modelled CO is defined by the same 14 regions as defined in the GFED project (see Fig.1). These contributions cannot be directly compared with observations because SOFT-IO only models contributions from recent emissions (and not older contributions nor the background mixing ratio). SOFT-IO is therefore used here as a qualitative tool to assess whether the modelled contributions are mainly due to anthropogenic or biomass burning emissions and to label the corresponding observed plume as such.

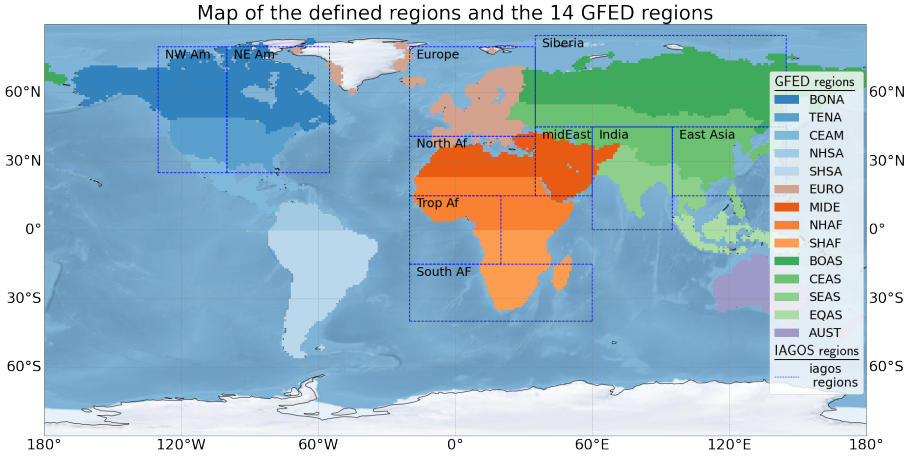

Figure 1. Map of the IAGOS regions (dotted lines) and the GFED defined regions (in colour)

In addition to the various observed parameters and to the SOFT-IO products, the IAGOS Data Centre provides some meteorological fields from the ECMWF operational analysis interpolated along the IAGOS flight track, as ancillary data (https://doi.org/10.25326/3) . Among these parameters (potential temperature, planetary boundary layer height potential vorticity), the potential vorticity (PV) is used to define whether the CO observations are above or below the dynamical tropopause (defined at 2PVU as in Thouret et al. (2006); Cohen et al. (2018)).

https://doi.org/10.5194/egusphere-2023-2949
Preprint. Discussion started: 15 January 2024

2.3 Methods

2.3.1 Regions and seasons

In order to synthesise the seasonal and regional characteristics of the CO anomaly, the observations from IAGOS are split in different regions. These regions are defined to be characteristic of specific meteorological and chemical regimes (sources of precursors) similar to Cohen et al. (2018). This study is dedicated to the higher values of the CO distribution, so the sizes of the regions are larger here in order to increase the number of data points per region and not miss any extreme event. By nature, as IAGOS uses commercial aircraft to sample the atmosphere, the different regions are not sampled equally over the same time period (see Fig.A1), but a minimum of 1500 flights per region over the full sampling period is respected.

Fig.1 shows the 10 regions defined and used in this study (dotted line). In addition, the colours of the map indicate the regions as defined by GFED which are used to assign an origin to the emitted CO (see 2.2). Fig.A1 in the appendix shows the availability of the data in each region. The number of flights is maximum over Europe due to the history of IAGOS and the dense traffic between the US and Europe, however since 2006, regular flights from Europe to South Africa have been added. In addition, regular flights to eastern and equatorial Asia have been added since 2012.

In the northern hemisphere mid-latitudes (NW Am, NE Am, Eur, Sib and E Asia), four periods of three months are defined according to the meteorological seasons (DJF, MAM, JJA, SON). Note that this study focuses only on the boreal summer and winter periods, one characterising the maximum of CO due to anthropogenic emissions in winter and the other one the maximum of forest fire activity in summer (section 3.1). The two transitional periods are not presented here as we focus on the influence of the biomass burning emissions on the CO signal. In Africa, the seasons are defined according to the shift of the ITCZ and the rainy seasons (as defined in Lannuque et al. (2021)) : DJFM and JJASO. The results for the two transitional periods (April-May and November) are not presented here. For the Middle-East, seasons of interest for this study are defined the same way as for Africa, because DJFM and JJASO there, also correspond to the maximum and minimum of the CO seasonal cycle, respectively (Figs.B1 and C1). Furthermore, the Middle-East is connected to Africa in terms of emissions as seen in Fig.1 (section 3.3). India (as defined Fig.1) is also an interesting region regarding the different influences of biomass burning and anthropogenic emissions from the different continents. Differently from Northern mid-latitudes and Northern Africa or Middle-East, the four seasons will be discussed here for India (section 3.2).

Finally, in order to characterise these CO extremes at different altitudes, the data sets are divided into three vertical layers.

- Lower Troposphere (LT): from the surface to 2000 m.
- Middle Troposphere (MT): from 2000 m to 8000 m.
- Upper Troposphere (UT): Above 8000 m and below the dynamical tropopause (defined as 2 PVU Thouret et al. (2006); Cohen et al. (2018)).

IAGOS samples the lower and free troposphere during the landing and take-off of commercial flights. Petetin et al. (2018a) showed that close to the surface, the IAGOS measurements are representative to urban areas and provide similar measurements

https://doi.org/10.5194/egusphere-2023-2949
Preprint. Discussion started: 15 January 2024

compared to city station facilities. At higher altitude, the samples are less influence by local emissions and therefore are representative of regional background conditions.

2.3.2 Definition of the CO anomalies

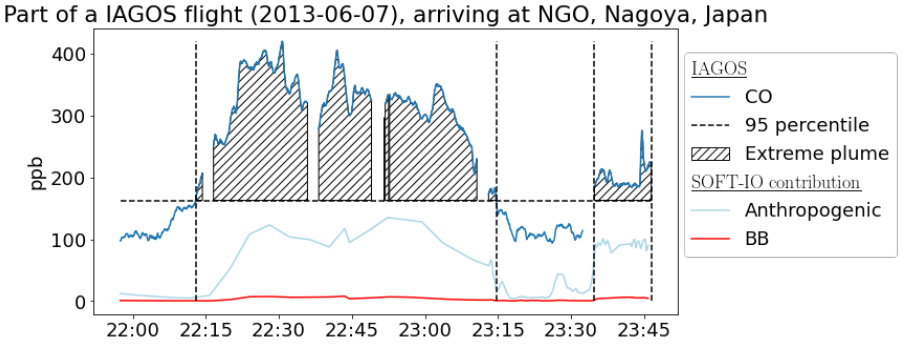

Figure 2. Illustration of the method used to define the CO anomalies applied to a IAGOS flight. The blue line represents the CO measured by IAGOS. The dashed line represents the seasonal and regional 95th percentile of the IAGOS dataset, it is used as a threshold for the CO anomalies in this study. The hatched area represents the anomalies. The light blue and red lines represent the modelled anthropogenic and biomass burning contributions modelled by SOFT-IO.

Fig.2 illustrates the detection of two plumes in the IAGOS observations. The CO anomalies are defined as CO values exceeding the threshold for three consecutive measurements (i.e. a distance of approximately 3 km during cruise phase). The chosen threshold used in this study is the 95th percentile (q95) calculated for each region/season/altitude range (see table 1).

Only data considered as CO anomalies are examined here. The selection process is repeated for each flight.

SOFT-IO is then used as a qualitative tool to assign a source type to each of the detected anomalies. This diagnostic is only applied if the contributions modelled by SOFT-IO are above a detection threshold defined as 5 ppb. Several thresholds were tested during this study and did not have a significant impact on the results. According to the method used in Petetin et al. (2018b) the four categories are defined as follow :

- Anthropogenic: if the anthropogenic contributions calculated by SOFT-IO are at least twice those of the biomass burning.
- Biomass burning (or wildfire): if the biomass burning contributions calculated by SOFT-IO are at least twice the anthropogenic contributions.
- Mixed sources: if none of the contributions, as calculated by SOFT-IO, is twice the other.
- Observed by IAGOS but undetected by SOFT-IO.

In Fig.2 both plumes of high CO mixing ratios are clearly attributed to anthropogenic sources. In addition, SOFT-IO provides information on the emitting region of the contributions (see section 2.2). This diagnosis is repeated for each plume detected. Thus, we can compute the main emitting region responsible for all detected plumes.

https://doi.org/10.5194/egusphere-2023-2949
Preprint. Discussion started: 15 January 2024

		LT	FT	UT
NW Am	DJF	256 ppb	160 ppb	146 ppb
	MAM	255 ppb	170 ppb	171 ppb
	JJA	251 ppb	149 ppb	145 ppb
	SON	243 ppb	141 ppb	120 ppb
NE Am	DJF	264 ppb	159 ppb	126 ppb
	MAM	246 ppb	166 ppb	156 ppb
	JJA	241 ppb	156 ppb	132 ppb
	SON	241 ppb	140 ppb	112 ppb
Eur	DJF	332 ppb	158 ppb	126 ppb
	MAM	267 ppb	164 ppb	140ppb
	JJA	200 ppb	140 ppb	123 ppb
	SON	253 ppb	138 ppb	109 ppb
Sib	DJF	no data	no data	127 ppb
	MAM	no data	no data	146 ppb
	JJA	no data	no data	181 ppb
	SON	no data	no data	123 ppb
E Asia	DJF	559 ppb	209 ppb	129 ppb
	MAM	504 ppb	265 ppb	185 ppb
	JJA	441 ppb	173 ppb	162 ppb
	SON	457 ppb	180 ppb	159 ppb
India	DJF	424 ppb	157 ppb	132 ppb
	MAM	305 ppb	191 ppb	130 ppb
	JJA	267 ppb	134 ppb	131 ppb
	SON	470 ppb	150 ppb	150 ppb
North Af	DJFM	no data	no data	145 ppb
	AM	no data	no data	156 ppb
	JJASO	no data	no data	110 ppb
	N	no data	no data	124 ppb
Middle E	DJFM	253 ppb	148 ppb	135 ppb
	AM	272 ppb	143 ppb	131 ppb
	JJASO	300 ppb	129 ppb	113 ppb
	N	244 ppb	127 ppb	118 ppb
Gulf of G	DJFM	724 ppb	297 ppb	190 ppb
	AM	419 ppb	203 ppb	171 ppb
	JJASO	280 ppb	192 ppb	147 ppb
	N	383 ppb	199 ppb	155 ppb
South Af	DJFM	219 ppb	132 ppb	172 ppb
	AM	272 ppb	120 ppb	148 ppb
	JJASO	400 ppb	245 ppb	197 ppb
	N	247 ppb	150 ppb	153 ppb

Table 1. q95 values used as thresholds for the different regions.

https://doi.org/10.5194/egusphere-2023-2949
Preprint. Discussion started: 15 January 2024

3 Results:

The first part of the results is dedicated to the five Northern hemisphere mid-latitude regions (NW Am, NE Am, EU, Sib and EAsia), then India, and Africa plus Middle-East. Each vertical layer will be treated one after the other from the lower troposphere to the UT (note Siberia is only sampled in the UT). The characteristics of the CO-extreme plumes will be given before presenting the associated O_3 distributions in such plumes.

3.1 Northern Hemisphere mid-latitudes

3.1.1 Lower troposphere (LT)

In the LT (Fig.3) of most regions the distribution of CO is higher in DJF than in JJA due to the higher anthropogenic emissions during the winter months (e.g mean of the anthropogenic emissions from CEDS2 in Europe are 60% higher in DJF than in JJA). The higher levels of CO near the surface in winter are also due to the weak convection and mixing in this season, which allows pollutants to accumulate in the boundary layer (Cohen et al., 2018). As expected, anthropogenic contributions have strong local influence in the LT (Fig. 3.c). For example, anthropogenic contributions are almost only from local sources in NW America and NE America in the LT, This is also true for Europe, where more than 86% of the anthropogenic contributions come from locally emitted near-surface sources. In DJF, as there are almost no wildfires in the northern hemisphere mid-latitudes almost all of the CO anomalies are attributed to anthropogenic emissions. In JJA even if they remain rare, some regions have a few of their anomalies attributed to Biomass Burning (BB) emissions. Those emissions are in the vast majority from Boreal regions, even in Europe where more than half of the BB contributions of the mix and BB anomalies are from Boreal North America.

As outlined in the introduction, CO is an interesting tracer for surface influenced air masses, but also because it is a precursor of O_3. It is therefore important to also analyse the O_3 mixing ratio within the detected CO plume. This is shown in Fig.4. This figure compares the seasonal distribution of O_3 measured in the 19 years of data to the values of O_3 measured in the different types of CO anomalies.

In the LT in DJF our results are similar regardless of the region. We observe values of O_3 inside the CO anomalies close to the minimums of the seasonal O_3 cycle. We can see that, in addition to the low photochemical activity linked to the boreal winter, we are seeing a cycle of O_3 destruction in the CO-rich fresh air masses. In JJA, the mean O_3 mixing ratios in the CO anomalies are closer to the median. However, there is strong regional variations showing the important local influence at this altitude.

https://doi.org/10.5194/egusphere-2023-2949
Preprint. Discussion started: 15 January 2024

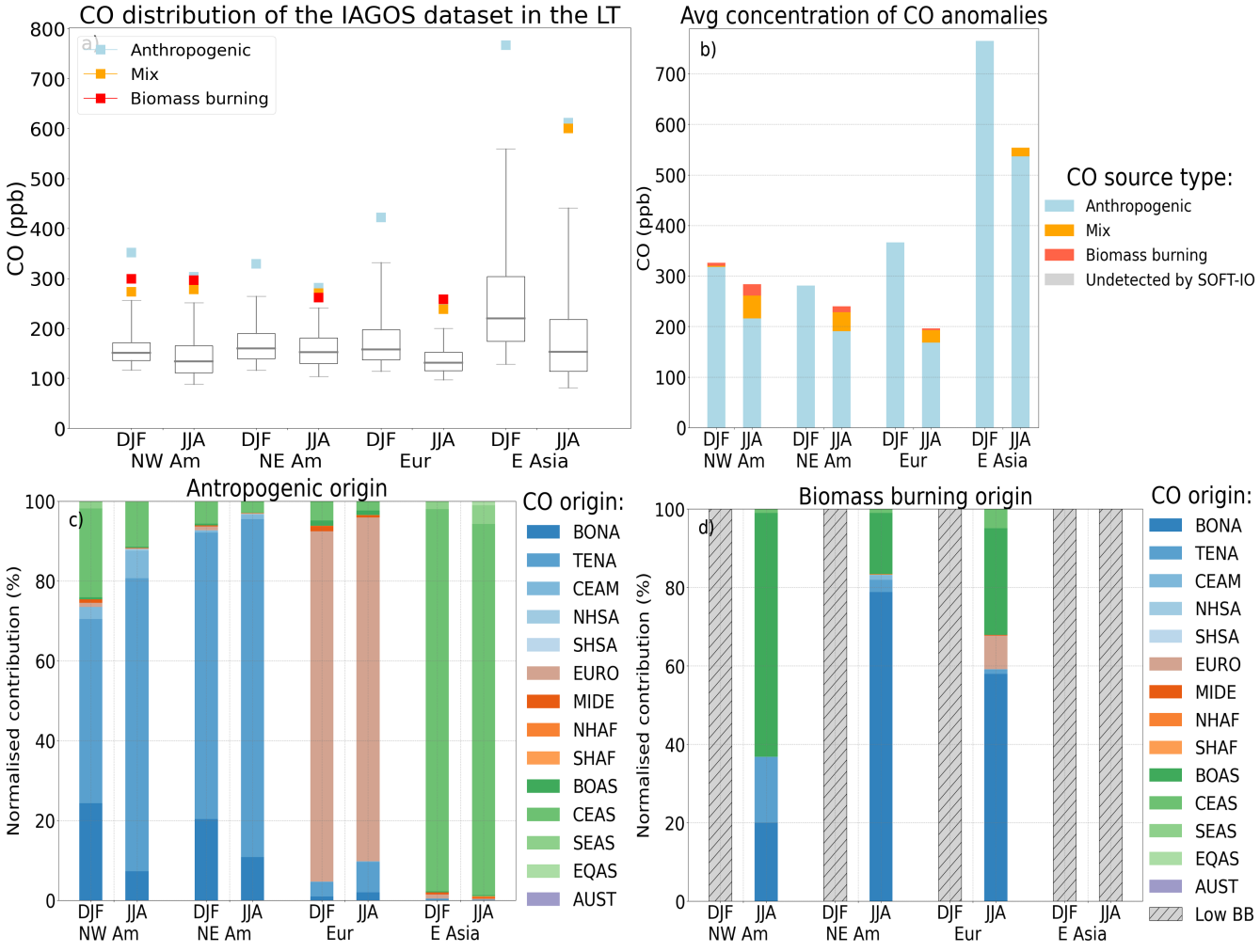

Figure 3. a) CO measured by IAGOS in the LT (below 2km). The box plot represents the 5th, 25th, 50th, 75th and 95th percentiles of the CO distribution, while the coloured squares represent the mean values of CO inside the detected anomalies (each colour represents a type of CO anomaly attributed to a different source with SOFT-IO: red for biomass burning, blue for anthropogenic and orange for mix sources). b) Bar plot showing the averaged mixing ratios of CO in all the detected anomalies (>q95) in the LT in each region for JJA and DJF (given by the total height of the bar), and their proportion according to the different sources (blue for anthropogenic, red for biomass burning and orange for mix, the relative height of the coloured blocks represents the proportion of each type of anomalies). The proportion of plumes where no contribution is modelled by SOFT-IO are represented in grey (in this figure no anomalies are undetected by SOFT-IO over the 4804 observed). c) Regional origin (according to GFED regions, as in Fig. 1) of the anthropogenic contributions of the anomalies associated with mix and anthropogenic sources in the LT in NH extra-tropics (the hatched part cover region/season with not enough anomalies attributed to the mixed or anthropogenic categories) d) Same for the origin of the biomass burning contributions associated with mix and biomass burning anomalies.

https://doi.org/10.5194/egusphere-2023-2949
Preprint. Discussion started: 15 January 2024

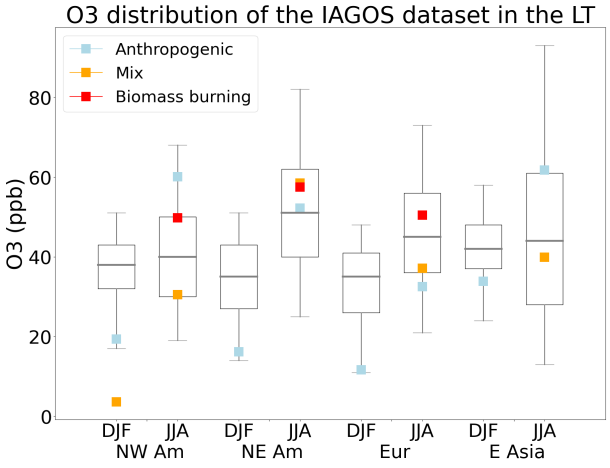

Figure 4. O_3 distribution measured by IAGOS in the lower troposphere (LT) (from the surface to 2000m). Coloured points represent O_3 mixing ratios inside the detected CO anomalies (each colour represents a type of CO anomaly attributed to a different source with SOFT-IO). The box plot represent the 5th, 25th, 50th, 75th and 95th percentile of the O_3 distribution of the complete database (of these regions, seasons and vertical layer) during the studied period with the simultaneous CO records.

https://doi.org/10.5194/egusphere-2023-2949
Preprint. Discussion started: 15 January 2024

3.1.2 Middle Troposphere (MT)

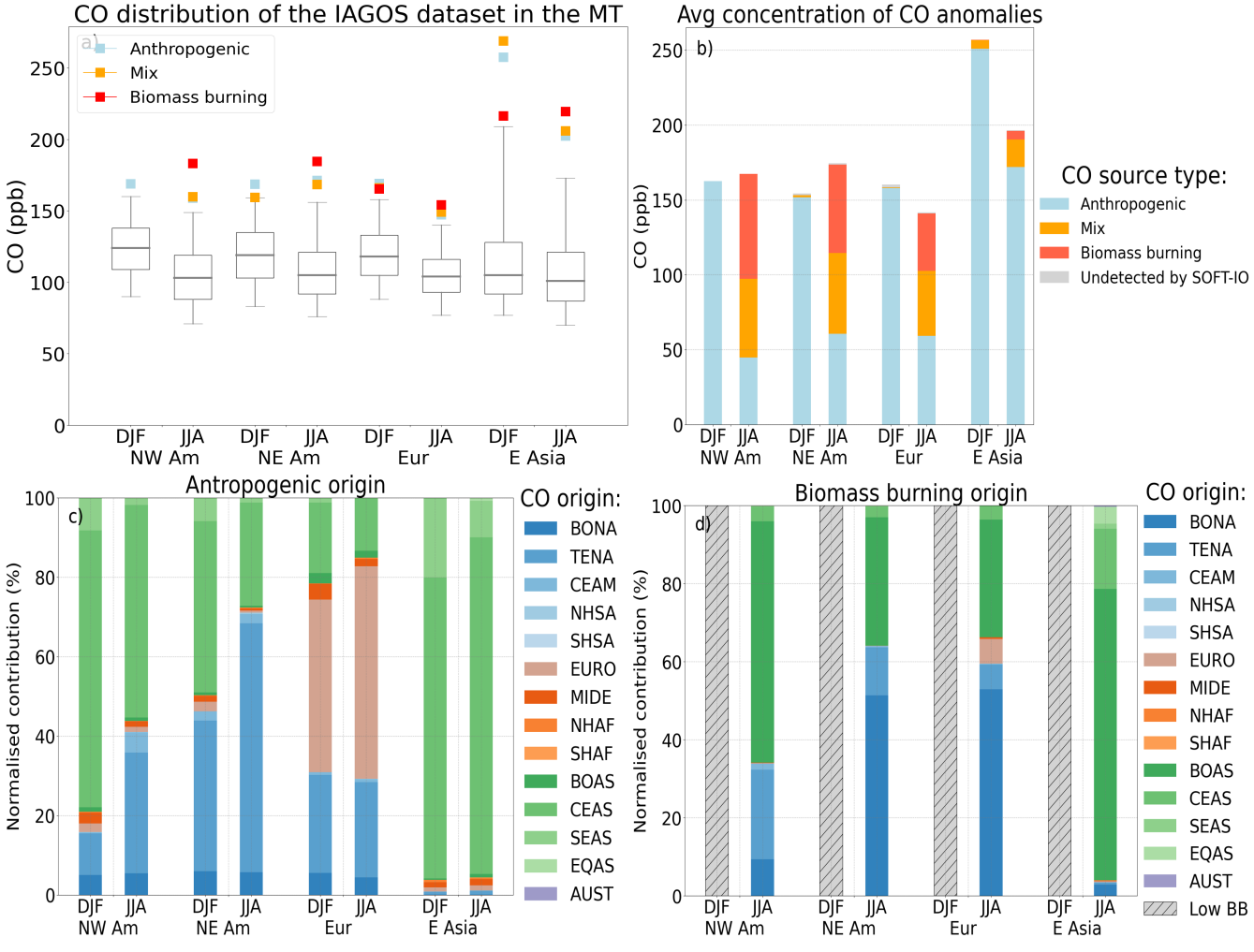

Figure 5. Same as Fig.3 but for the MT (between 2000m and 8000m). At this altitude 24 anomalies over the 5341 observed, are undetected by SOFT-IO, representing thus 0.4% (in grey on panel b).

In the MT (Fig.5) the CO distribution present a maximum in winter in the CO distribution. However, the amplitude of the seasonal cycle of the anomalies is lower than in the LT. Indeed, the effect of the high anthropogenic emissions in DJF is counterbalanced by the increased number of convective episodes and the higher overall vertical transport during JJA which tend to increase the CO mixing ratio in the MT during the summer months. In this layer of the atmosphere the local influence in the anthropogenic contributions (Fig.5.c) is still strong. The SOFT-IO modelled contributions in NW America are mostly coming from Asian emissions whereas contribution in the eastern part comes mostly from north America. In Europe however, the anthropogenic contribution comes at 40% from Europe and the rest is split between America and Asia. BB contributions

https://doi.org/10.5194/egusphere-2023-2949
Preprint. Discussion started: 15 January 2024

comes in the vast majority from Boreal America and Asia. We also note the increased number of episodes attributed to either BB emissions or mixed sources in the MT of America and Europe in JJA (Fig.5.b). In JJA, the plume attributed to BB emissions are the most intense. SOFT-IO is modelling the origin of the BB contribution to come in the vast majority from the Boreal regions of Asia and America (Fig.5.d). Those anomalies in JJA are the most intense in the four regions studied here (Fig.5.a).

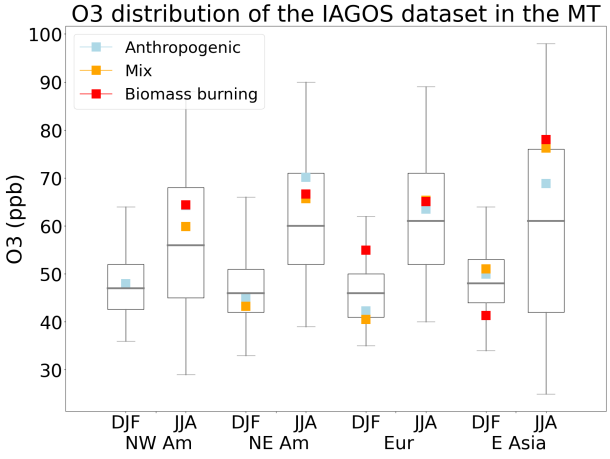

Figure 6. Same as Fig.4 for the MT

Fig.6 shows the volume mixing ratio (vmr) of O_3 associated with high values of CO. In the MT there is almost no signal during the winter months (mixing ratio of O_3 inside CO anomalies is close or below the median) because of the relatively weak photochemical activity. In JJA the O_3 mixing ratio within the CO anomalies is between the median and the 75th percentile of the total O_3 distribution.

https://doi.org/10.5194/egusphere-2023-2949
Preprint. Discussion started: 15 January 2024

3.1.3 Upper troposphere

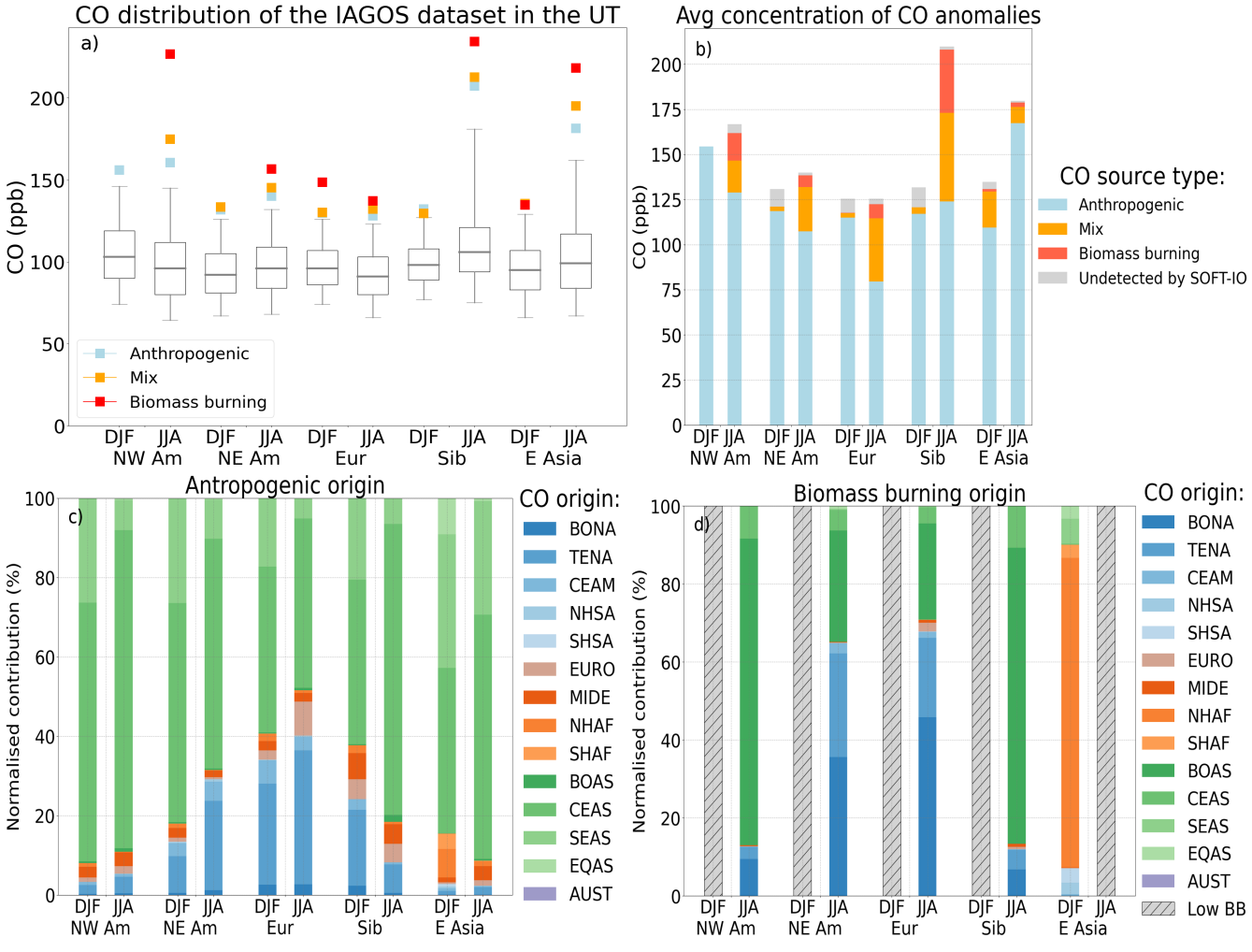

Figure 7. Same as Fig.3 but for the UT (between 8000m and the dynamical tropopause (2PVU)). At this altitude 223 anomalies over the 7865 observed are undetected by SOFT-IO, representing thus 2.8% percent (in grey on panel b).

Figs.7 are the same figures as Figs.3 for the upper tropospheric layer. Some regions like Europe do not show important variations of their 95th percentile between JJA and DJF while other regions like Siberia and East Asia present a drastic increase during JJA.

We can see on Fig.7.b that in DJF the majority of the plumes are explained by anthropogenic emissions. In JJA, the number of anomalies attributed to BB increases with the onset of the northern hemisphere fire season. However, a higher number of anomalies are still explained by anthropogenic emissions, which is different from what we observe in the MT of America and Europe. This is because the most intense pyroconvection episodes from boreal fires rarely reach the UT directly (Labonne et al.,

https://doi.org/10.5194/egusphere-2023-2949
Preprint. Discussion started: 15 January 2024

2007). Thus, regardless of the emission intensity, vertical transport is required for a CO plume to reach the UT. Anthropogenic emissions continuously inject CO into the boundary layer. Consequently, episodes of significant vertical transport of air masses from the surface to the UT may cause a drastic increase in the upper tropospheric CO mixing ratio, even if local emissions are not higher than usual.

However, due to the intensity of BB emissions, when these plumes reach the UT they often are the most intense CO anomalies (Fig. 7.a). The most intense ones are detected in north-western America, Siberia (and East Asia in small proportion) and they are attributed to emissions of biomass burning from Boreal Asia. In the UT, those anomalies even if not the most frequent are extremely intense. Siberia and East Asia both present two of the most important amplitude of the CO seasonal cycle. The large increase of CO in JJA in Siberia with respect to DJF can be partly attributed to the local wildfire. However, approximately 60% of the episodes are still related to anthropogenic emissions and around 25% are due to mixed sources. The mean mixing ratio of these episodes during the summer months also increased significantly. Furthermore, East Asia shows a similar summertime increase in the mixing ratio of its extremes without a significant number of BB plumes.

In DJF in Siberia, the anthropogenic contributions are small and there is no clear signal. In JJA however, there is a 50% increase in the anthropogenic contribution, of which 70% comes from CEAS. The low mixing ratio and contribution in winter are partly explained by the presence of the Siberian high, which prevents the export of polluted surface air masses from the eastern part of Asia (Pochanart et al., 2004).

However, the wind direction changes with the onset of the East Asian summer monsoon. In JJA, there are strong southeasterly ascending winds that transport pollution and moisture into the upper troposphere of East Asia and these air masses can even reach the northern part of Siberia. It can explain the very low number of episodes associated with wildfires emissions (mixed and BB) in East Asia as heavy rainfall prevents wildfires in this region and the prevailing winds from the Pacific ocean are less likely to bring air masses polluted by Siberian fire (Pochanart et al., 2004). In the other regions (North America and Europe), the most intense anomalies remain the one attributed to BB emissions and they represent around 5 to 10% of the number of anomalies. As we said previously the BB anomalies in NW America are attributed to emission from Boreal Asian wildfires. In NE America and Europe those anomalies are less intense and they are attributed to wildfires from Boreal America, Boreal Asia and Temperate North America. In a lot of regions most of the emissions from BB are from the two boreal regions (Boreal America and Boreal Asia), which is probably due to the higher emissions height of those fires increasing the probability of the emitted CO to reach the UT.

In the two regions of North America, the main anthropogenic contributions to CO anomalies come from CEAS, but it can be seen that the influence of American emissions is greater in the eastern part, while the contributions in the western part are almost entirely coming from CEAS. Europe's anthropogenic contributions come equally from Asia and North America. Only a small fraction is emitted locally, which is not surprising given the relatively weak convective activity in the region.

The main result is the importance of the contribution from Asia (green colours) which represents an important part of the total contribution in every region. Within the Asian contribution, the CEAS contributions are the most important. CEAS alone accounts for at least 40% of the anthropogenic contribution in the different regions and even reaches 79% in WNam, where the total emissions during this period account for about half of the northern hemisphere emissions. As a comparison,

https://doi.org/10.5194/egusphere-2023-2949
Preprint. Discussion started: 15 January 2024

North American emissions represent approximately 15% of the northern hemisphere emissions but only 14% of the modelled anthropogenic contributions in the different regions. It means that "high level" emissions are not the only parameter to take into account, but there is also the fact that the East Asian atmosphere benefits from strong convective activity, which allows the polluted air to be quickly transported into the UT where it can be distributed all over the Northern hemisphere. There is also the presence of the Tibetan plateau, which can play an important role by lofting polluted air mass into the upper part of the troposphere (Bergman et al., 2013; Pan et al., 2016).

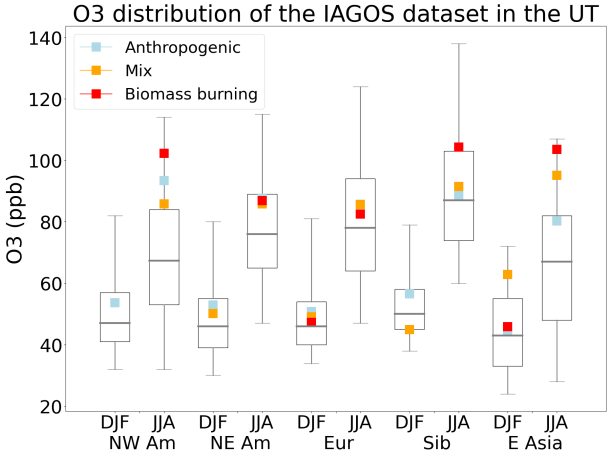

Figure 8. Same as Fig.4 for the UT.

Mixing ratios of O_3 within CO anomalies are shown in Fig. 8. As explained in sect. 2, the UT is defined as being below the 2 PVU surface. It may therefore include some stratospheric air or at least part of the mixing layer. The O_3 shown Fig. 8 are mostly typical of tropospheric values, but it is possible that a small fraction of them are contaminated by some stratospheric air masses. Obviously, O_3 presents a stronger seasonal cycle than CO (Fig. 8). In DJF, the O_3 mixing ratio is at its minimum and values within the anomalies of CO are slightly lower than the 75th percentile in most regions. However, during the summer months the regional variations are more important, some regions show values of O_3 between the 75th and 95th percentile inside the CO anomalies whereas in Europe for example the O_3 values are just above median level.

The CO anomalies with the most intense values of O_3 are the anomalies associated with BB emissions from Boreal Asia and detected in : NW America, East Asia and Siberia. We saw that those fires were responsible for particularly intense CO anomalies and so probably emitted not only CO but also many reactive compounds such as VOCs and NOx which are other precursors of O_3. As for episodes associated with anthropogenic emissions, their associated mixing ratios of O_3 are often above median levels but a lot of variation can be observed depending of the regions. In NW America, in JJA levels of O_3 inside the anthropogenic CO anomalies are high (93ppb so 10ppb above its 75th percentile), those anomalies are associated with emission from CEAS, so the air mass rich in pollutant had the time to produce important quantity of O_3 before reaching the American continent.

https://doi.org/10.5194/egusphere-2023-2949
Preprint. Discussion started: 15 January 2024

3.2 India

The seasonal cycle of CO over India is characterised by a minimum in JJA in the LT and MT, and a maximum in SON-DJF in the LT superposed by a maximum in MAM in the MT (Fig.D1 and E1). Indeed, the Asian monsoon has a strong influence in this part of the world on the redistribution of the pollutants emitted at the surface. Interesting and specific features appear in all four seasons in the UT as highlighted in Fig.9. DJF and MAM have a similar signal in the UT as the same sources are at the origin of most of the CO anomalies. We can see on Fig.9.b that half of the CO anomalies are linked to BB emissions (pure BB and mix sources) and half are pure anthropogenic anomalies. From December until late March, it is the fire season in the Northern Hemisphere of Africa, and we can see on Fig.9.d that those emissions can reach the UT of India. The anthropogenic CO anomalies receive an influence from CEAS and SEAS but also from NHAF.

In JJA, it is the wet phase of the monsoon in India and almost all the CO anomalies are caused by anthropogenic emissions from India or the close proximity (SEAS and CEAS). In SON, the CO anomalies are at their maximum and are caused by anthropogenic emissions from SEAS and CEAS but also by BB emissions from EQAS. The BB anomalies are cleary the most intense during this season. It is interesting to note that in the vast majority those BB anomalies have been recorded by IAGOS in 2015. This year was hit by an important El Niño phenomenon caracterized by especially intense fires over the Equatorial part of Asia.

https://doi.org/10.5194/egusphere-2023-2949
Preprint. Discussion started: 15 January 2024

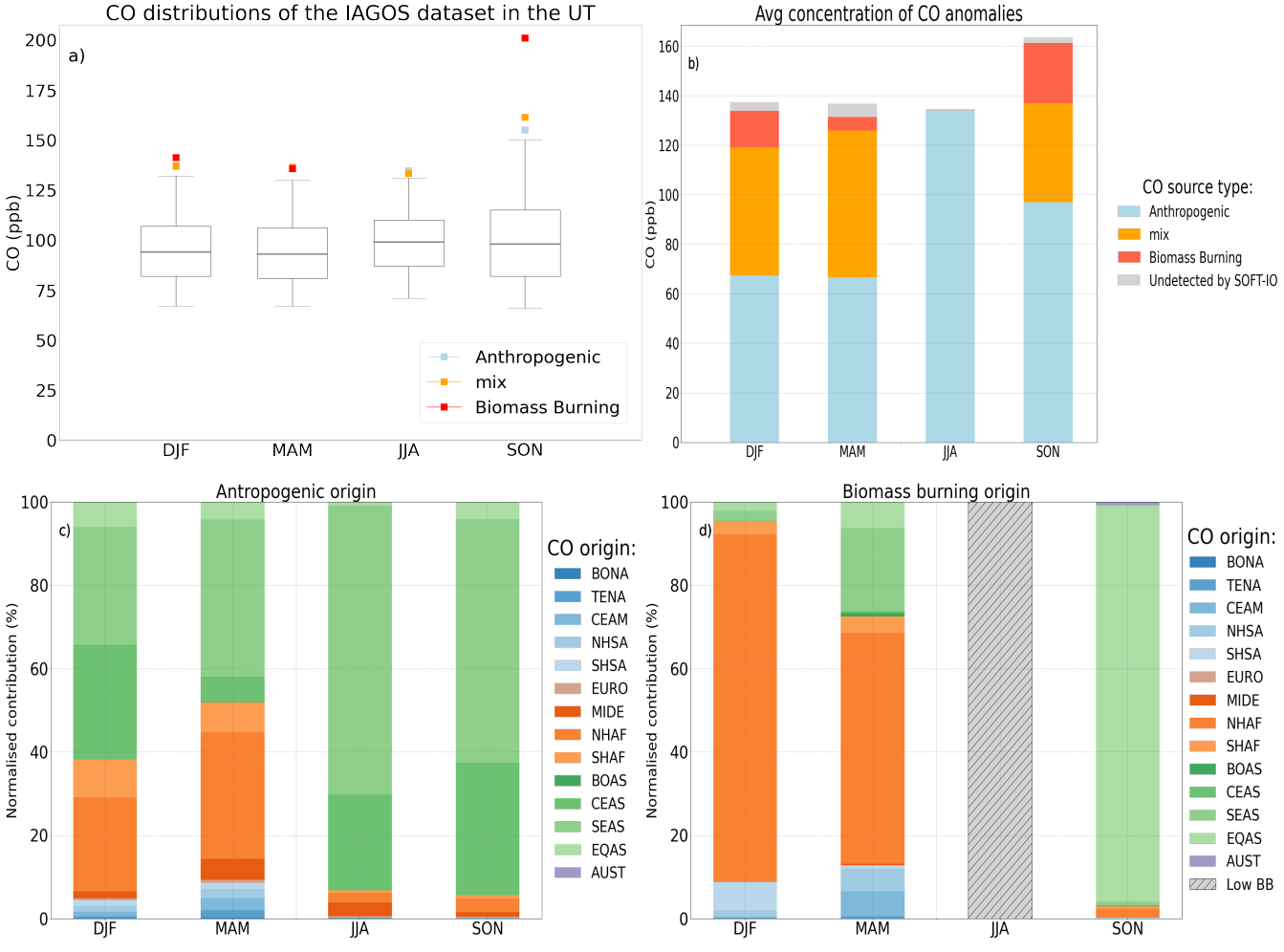

Figure 9. Same as Fig.3 but only for the Indian region during the four seasons for the UT (between 8000m and the dynamical tropopause). (In MAM in panel a) the other squares are superposed below the one from BB origins). At this altitude 37 anomalies over the 2228 observed are undetected by SOFT-IO, representing thus 1.7% (in grey on panel b).

During winter in India, around 50% of the plume originates from either mixed or biomass burning sources from Northern Africa. Fig 10 shows that the associated O_3 values present in these plumes are high (above the 75th percentile (62ppb)). The other half of the anomalies are from anthropogenic sources and their associated values of O_3 are drastically lower and close to the 25th percentile (41ppb). The anomalies measured during the months MAM have similar characteristics than the anomalies from DJF but this time the O_3 associated to the anthropogenic plumes are at the same level as the one from BB origins, they are all close to the 75th percentile (81 ppb). During this season O_3 is at its maximum and mixing ratios are similar to summer time O_3 values in the mid latitudes. Anomalies in JJA are caused by the local emission of anthropogenic CO rapidly transported to the UT by the important convective activity of the South Asian Summer Monsoon (SAMA). This rapid transport and the

https://doi.org/10.5194/egusphere-2023-2949
Preprint. Discussion started: 15 January 2024

relative small age of the air mass can explain that the associated values of O_3 are close to the median (65 ppb). In the post monsoon season (SON) BB anomalies from Equatorial Asia are added to the local anthropogenic anomalies. The values of O_3 in the BB plumes are low and close to the 25th percentile (44 ppb).

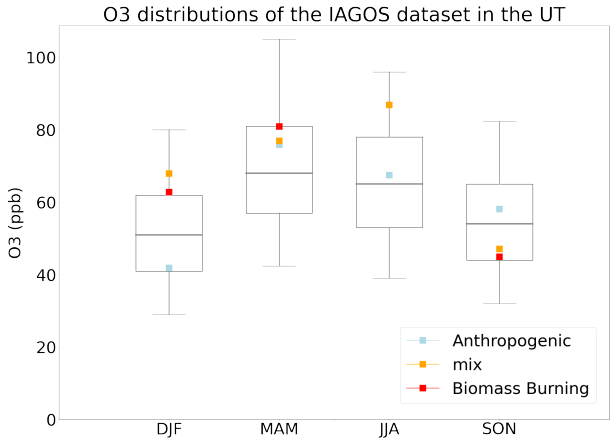

Figure 10. Same as Fig.4 for the UT in the Indian region during the four seasons.

https://doi.org/10.5194/egusphere-2023-2949
Preprint. Discussion started: 15 January 2024

3.3 Africa and Middle East

3.3.1 Lower and Middle Troposphere

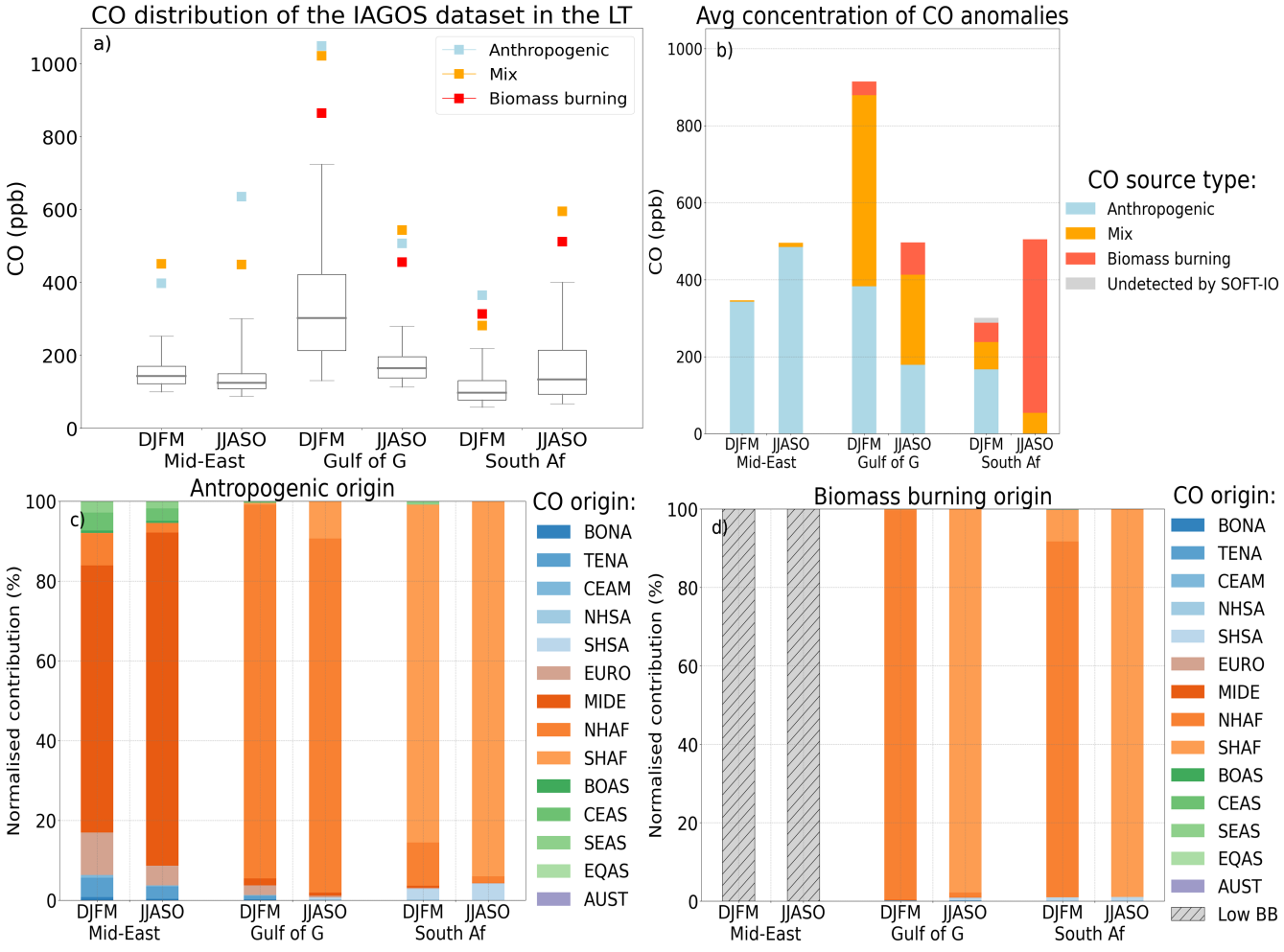

Figure 11. Same as Fig.3 but for the LT (below 2 000m) in Africa and Middle East. At this altitude 3 anomalies over the 1449 observed are undetected by SOFT-IO, representing thus 0.2% (in grey on panel b).

https://doi.org/10.5194/egusphere-2023-2949
Preprint. Discussion started: 15 January 2024

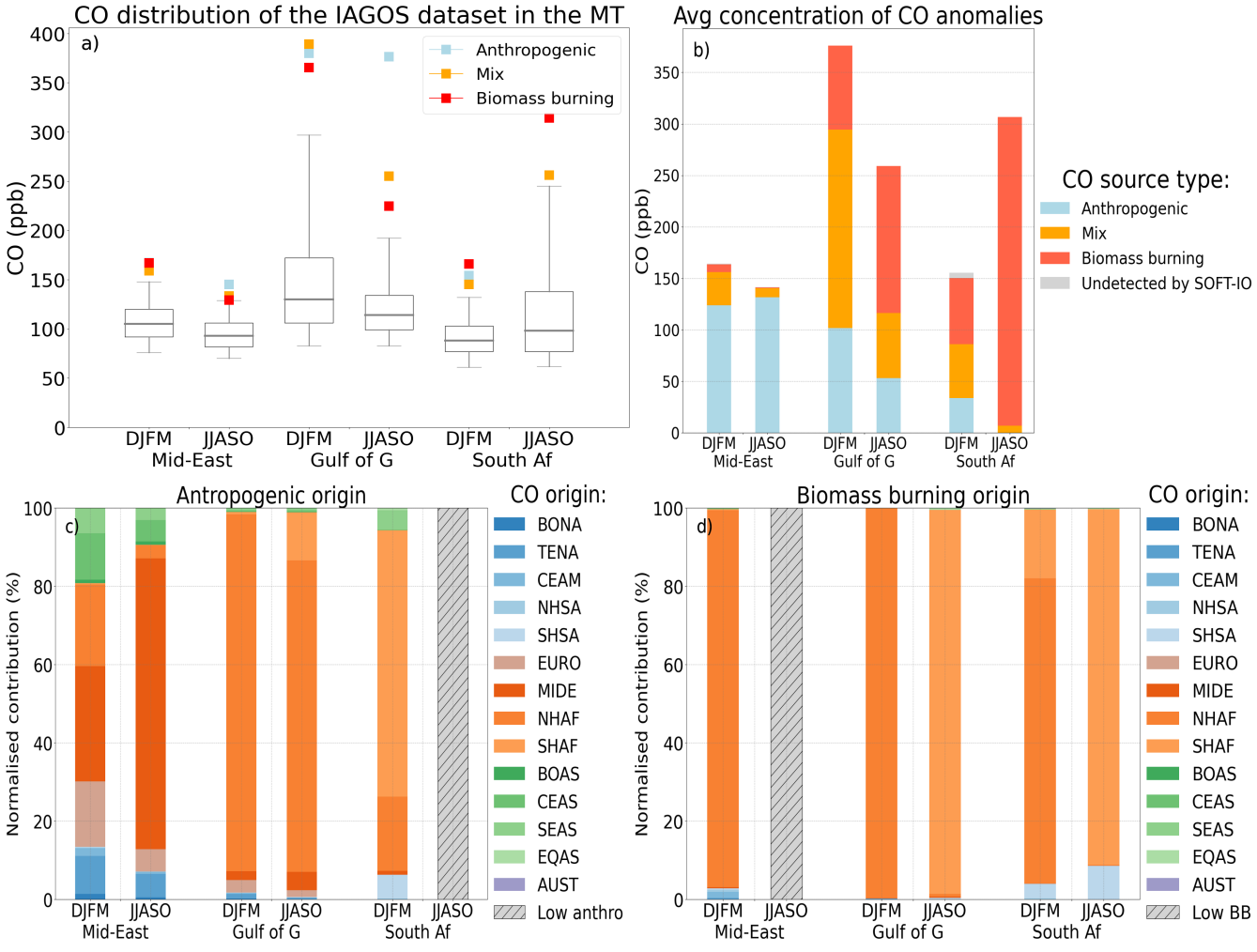

Figure 12. Same as Fig.3 but for the MT (between 2 000m and 8 000m) in Africa and Middle East. At this altitude 8 anomalies over the 1528 observed are undetected by SOFT-IO, representing thus 0.5% (in grey on panel b).

This section is focused on the CO anomalies detected over Africa and Middle East. As the result in the LT and in the MT present similar characteristics they are treated simultaneously.

Figs. 11.a and 12.a show the CO distribution in the two regions of Africa (Gulf of Guinea and Southern Africa) and the Middle East in the LT and the MT. Both layers present a maximum in DJFM in The Gulf of guinea with a 95th percentile above 724 ppb in the LT and 297ppb in the MT.

Indeed, DJFM is the dry season in the Northern part of Africa, which causes high levels of CO from biomass burning emissions (see Fig. 11.c). In the Gulf of Guinea, the plumes have higher values of CO in DJFM than in JJASO and the modelled contribution from SOFT-IO comes equally from anthropogenic sources and from wildfires. It is worth noting the increased proportion of BB sources in the MT. Obviously, the contribution of anthropogenic emissions maximize near the

https://doi.org/10.5194/egusphere-2023-2949
Preprint. Discussion started: 15 January 2024

surface, especially over the Gulf of Guinea (most of IAGOS aircraft arriving/departing from Lagos, Nigeria), one of the largest populated and polluted urban area of the continent. Higher in the troposphere (in the MT), the intensity of the CO anomalies attributed to anthropogenic sources decreases in favour of those from BB and mixed sources. These latter sources can come from further away and are more representative of the overall region (Petetin et al., 2018a).

The changes in origins of the BB contributions in DJFM and JJASO can be explained by the shift of the wildfires season from the northern hemisphere to the southern hemisphere. Moreover, our data are mostly centred around Lagos as it is the most sampled airport of the regions and in DJFM, trade winds blow from the north of Lagos as the ITCZ is located south of the city (e.g Nicholson (2018); Sauvage et al. (2005)). In JJASO, with the shift of the ITCZ trade winds follows so surface prevailing winds bring air masses from the south of LAGOS and the enhanced marine influence explains the overall reduction of the intensity of CO anomalies during this season.

In JJASO, during the dry season of southern Africa, the anomalies are the most intense there. The MT 95th percentile is just below 250 ppb in JJASO and most of its detected anomalies attributed to emissions from local fires.

The Middle East plumes are mostly originating from anthropogenic emissions during both seasons in the LT and the MT. Anthropogenic contributions are mostly emitted by the Middle East region itself (Fig. 11.c), except in DJFM in the MT, where anomalies may also be influenced by neighbouring regions :Europe, North Africa and North Asia.

Fig.13 and 14 show the O_3 distribution measured by IAGOS as well as its mixing ratio inside the detected CO anomalies. In the following paragraph if not mention otherwise the O_3 mixing ratio refers to the mixing ratio inside the CO anomalies. The box plot Fig.13 shows that the lower part of the troposphere present important variability between regions and seasons. In DJFM, in the Gulf of Guinea values of O_3 associated to the CO anomalies are just above the median in the LT, whereas it is almost as high as the 95th percentile in the MT. In JJASO, in the gulf of Guinea values of O_3 exceed the median only during the mix and BB anomalies in the MT.

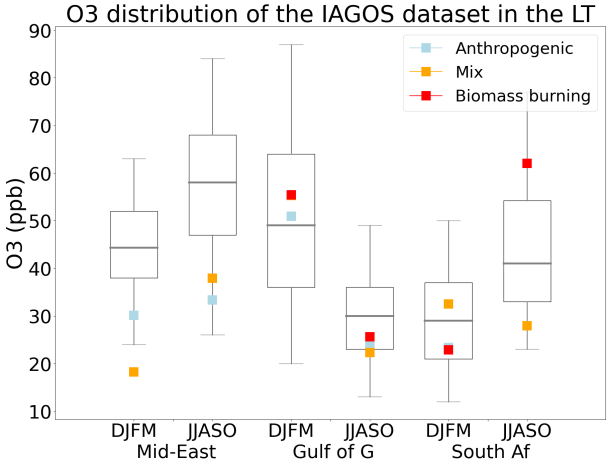

Figure 13. Same as Fig.4 for the LT in Africa and Middle East

https://doi.org/10.5194/egusphere-2023-2949
Preprint. Discussion started: 15 January 2024

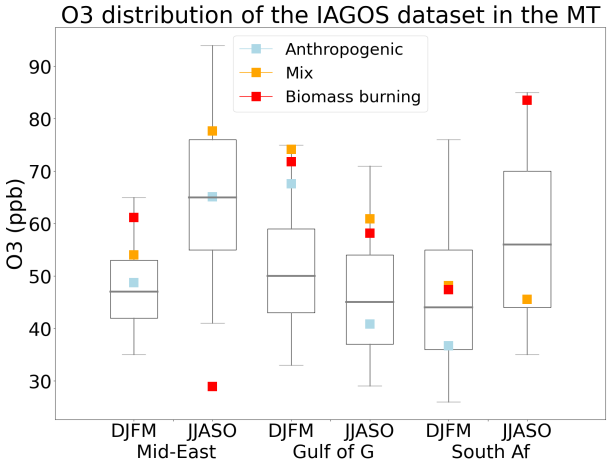

Figure 14. Same as Fig.4 for the MT in Africa and Middle East

In the Middle East, values of O_3 inside CO anomalies attributed to anthropogenic emissions are lower than the 25th percentile in the LT, which is similar to the observation made on the northern hemisphere mid-latitudes. In the MT, the anthropogenic anomalies are close to the median during both season. The anomalies attributed to mix and BB present values of O_3 higher than the 75th percentile during both seasons DJFM and JJASO.

South Africa present low values of O_3 in DJFM but much higher values during the wildfires season of the southern hemisphere. As in the Northern Hemisphere, the mixing ratio of O_3 inside plumes of CO influenced by wildfires is higher than the median. The important mixing ratio of O_3 in the BB anomalies where already discussed previously for the NH mid latitude CO anomalies and can be caused by the important quantity of reactive gases acting as O_3 precursors emitted by wild fires (e.g. Galanter et al. (2000); Mauzerall et al. (1998)).

3.3.2 Upper troposphere

As the seasonality of CO in the African upper troposphere has already been described in Lannuque et al. (2021), this section will emphasise the differences between the CO seasonal cycle presented in Lannuque et al. (2021) and the CO extreme values presented here.

https://doi.org/10.5194/egusphere-2023-2949
Preprint. Discussion started: 15 January 2024

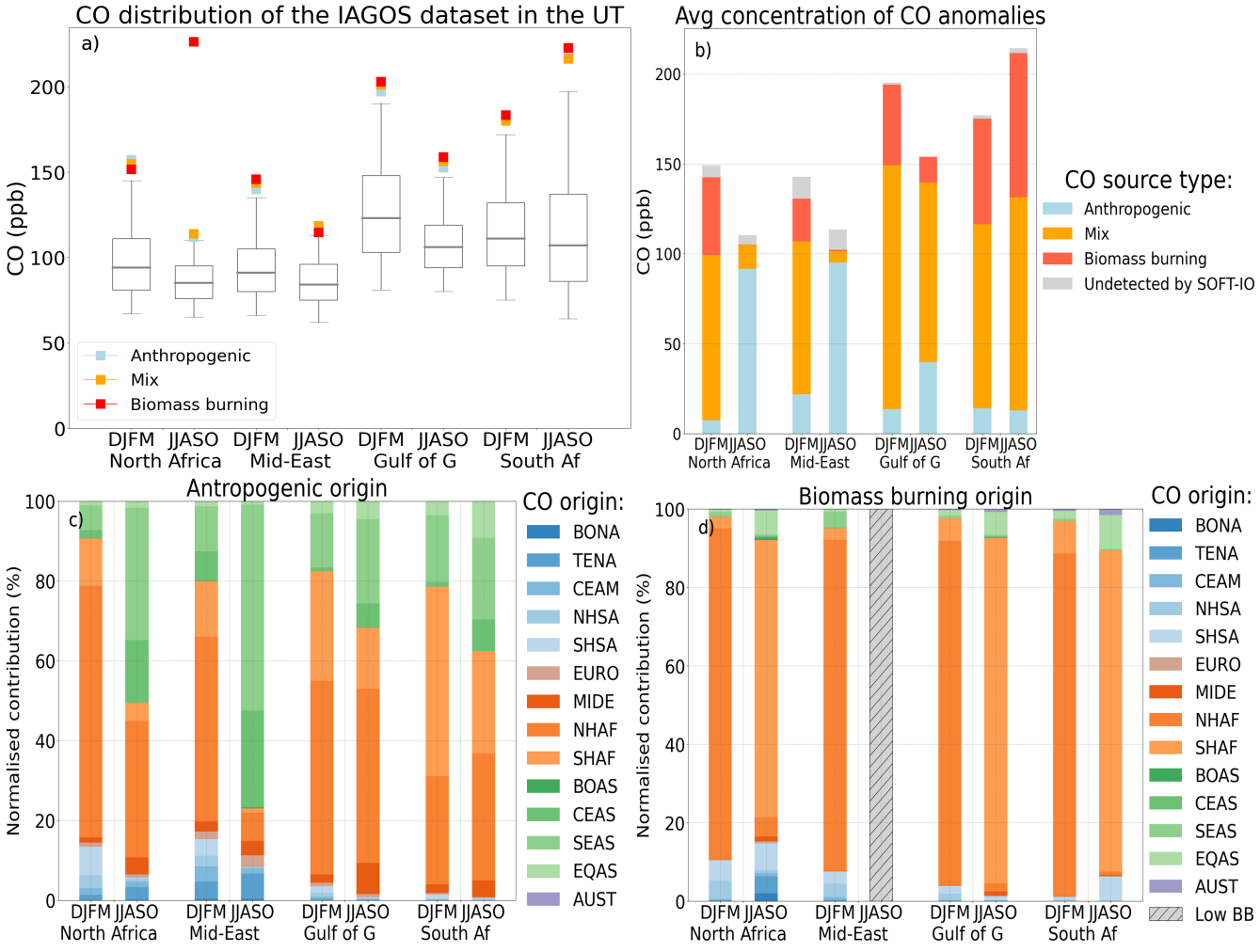

Figure 15. Same as Fig.3 but for the UT (between 8000m and the dynamical tropopause) in Africa and Middle East. At this altitude 268 anomalies over the 5859 observed are undetected by SOFT-IO, representing thus 4.6% (in grey on panel b).

Similarly to the study of the CO seasonal cycle from Lannuque et al. (2021), the anomalies are the most intense in the hemisphere of the strongest Hadley cell. In DJFM, the dry season is in the African Northern hemisphere causing important wildfires emitting a lot of CO, whereas in JJASO, the dry season is in the southern hemisphere and the most intense CO anomalies are detected in South Africa.

The Middle East and the North of Africa, similarly to the Gulf of Guinea show an important seasonal variation with a maximum in DJFM. Fig.15.b shows that the DJFM maximum reached in the northern hemisphere regions are mostly caused by important wild fires plumes from NHAF (Fig. 15.d). In JJASO, it is the wet season in NHAF, so BB emissions are drastically reduced in the region. Furthermore, similarly to the study of Lannuque et al. (2021), anthropogenic CO is transported from SEAS (Fig. 15.c). Indeed, there are significant anthropogenic emissions in the Indian subcontinent, and the active convection

https://doi.org/10.5194/egusphere-2023-2949
Preprint. Discussion started: 15 January 2024

brought by the Asian Summer Monsoon (ASM) allows the emitted CO to be rapidly transported from the surface to the UT. There, it is trapped in the Asian Monsoon Anticyclone (AMA) (Park et al., 2008; Barret et al., 2008; Tsivlidou et al., 2022).

Anomalies in the gulf of Guinea and in South Africa in the UT are heavily influenced by BB emissions, only 7% of the plumes in the gulf of Guinea are solely caused by anthropogenic emissions in DJFM. The others are caused by either pure BB emissions or mixed sources. The BB contribution comes from either NHAF or SHAF depending on the season. In DJFM, in Southern Africa it is interesting to note that the CO mixing ratio are higher in the UT than in the MT (Figs 12 and 15 and table1). It shows the importance of the Hadley cell circulation for the distribution of the pollutant in the UT.

The signal of the climatologies studied in Lannuque et al. (2021) and of the extreme studied here, is similar. The main differences are the increased BB proportion from NHAF in DJFM in the four regions. The small contribution from North America observed by Lannuque et al. (2021) is barely visible here as the air mass transported from there are probably too diluted (i.e. close to the median) to contribute to any important anomalies of CO.

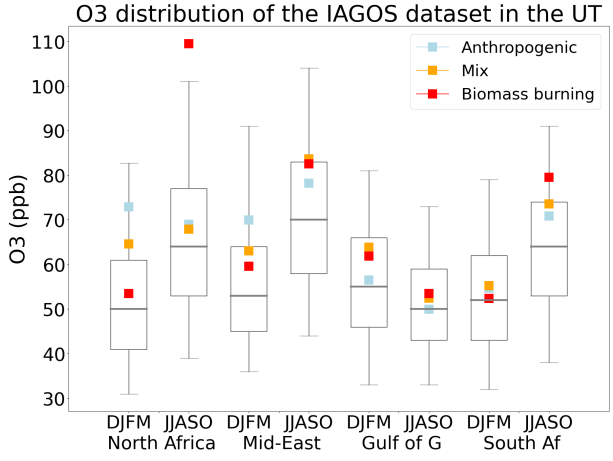

Figure 16. Same as Fig.4 for the UT in Africa and Middle East

O_3 mixing ratio associated to the observed CO anomalies is shown in Fig.16. The upper troposphere signal is not as clear as the one from the northern hemisphere. However, like in the MT in middle East and northern Africa , we can see that the O_3 mixing ratio in the BB anomalies are higher than the median of O_3 and can even reach the 75th percentile of O_3 in DJFM. In JJASO, because of the increased sunlight in the northern hemisphere the O_3 distribution is higher than in DJFM, but the mixing ratio of O_3 inside the anthropogenic CO anomalies are between the median and the 75th percentile in Northern Africa and Middle East (the BB and mix anomalies are extremely rare during JJASO in these regions).

In the gulf of Guinea, the overall distributions of O_3 measured by IAGOS is lower than in the rest of Africa. Its maximum values of O_3 are observed in DJFM during the wildfire seasons of North Africa. The O_3 values observed in the CO anomalies are a bit lower than the 75th percentile in DJFM and close to the median in JJASO. In Southern Africa, in DFJM, during the raining phase of the southern hemisphere, no clear signal is observed. In JJASO during the fires seasons O_3 is at its maximum and high values are observed in the CO anomalies.

https://doi.org/10.5194/egusphere-2023-2949
Preprint. Discussion started: 15 January 2024

4 Conclusions

This study is based on the in-situ IAGOS CO anomalies defined as the observations above the 95th percentile of each individual altitude range (LT, MT, or UT), region and season. In total, over the 18 years of measurements, more than 43,000 flights were made. In addition, SOFT-IO allows us to give a diagnosis on the main type of source as well as the region of emission responsible for the detected CO anomalies. As a reminder, SOFT-IO is based on FLEXPART retro-plumes initiated at each IAGOS measurement point. The back trajectory ensembles are then coupled to two CO emissions inventories : GFAS for the biomass burning and CEDS2 for anthropogenic emissions. The conclusions below relate only to CO anomalies (consecutive values of CO above the 95th percentile of the region/season/altitude).

At the northern mid-latitudes, anthropogenic emissions peak in winter, and biomass burning emissions peak in summer. The anomalies in the LT are very sensitive to local emissions which are highest during these winter months, and because of the weak convection and low photochemical activity in the northern hemisphere, these emissions accumulate until spring.

In the middle troposphere, the CO plumes over the NWam, NEam and Weur regions in JJA are mainly due to boreal fire emissions. Those fires originate either from boreal Asia or boreal America. CO plumes from anthropogenic origins still account for a significant proportion of the anomalies, but unlike the lower troposphere, the origins of these emissions are split between a local and a long-range influence.

For instance, a large proportion of the plumes over NWam originate from emissions in East Asia. In Europe, the majority of CO anomalies attributed to BB result from emissions in either boreal America or boreal Asia, with only 10% being due to fires on the European continent. East Asia continues to be dominated by anthropogenic pollution throughout the year, due to several factors. This is due to the high levels of anthropogenic pollution emitted in the region, as well as the favorable conditions for these emissions to rise out of the lower troposphere due to the high level of convective activity. Furthermore, the summer monsoon winds from the southeast do not frequently transport emissions from Asian boreal fires towards East Asia.

In the UT, in northern mid-latitudes, anomalies caused by BB emissions remain less frequent than the one caused by anthropogenic emissions, but they are consistently the most intense during the boreal fire season (JJA). During the summer months, the upper values of the CO distribution (75th percentile and higher) in siberian and East Asian regions experienced a significant increase. Around one third of the plumes identified above Siberia are associated with fire emissions. The rest are anomalies due to anthropogenic emissions from East Asia. This transport of pollution to Northeast Siberia is partly due to the East Asian monsoon, which transports air masses from Southeast Asia to Northeast Siberia.

The LT and the MT of the Indian troposphere are mainly influenced by local anthropogenic emissions. The UT, on the other hand, is influenced by different types of sources from different regions. In DJF and MAM, plumes linked to both anthropogenic and fire-related pollution are detected. The fire plumes come mainly from North African fires. Anthropogenic plumes, have both local, North African and East Asian origins. In JJA, and during the Indian monsoon, strong convective activity favours the export of local pollution to the UT and most plumes are therefore attributed to local anthropogenic pollution. Finally, during the SON months, the plumes are linked both to anthropogenic pollution from South and East Asia and to pollution linked to fires from equatorial Asia. The El Niño episode in 2015 and the major fires that took place during the year in equatorial Asia

https://doi.org/10.5194/egusphere-2023-2949
Preprint. Discussion started: 15 January 2024

had a major influence on our measurements, since most of the fire plumes seen during the SON months in India were detected during that year.

CO anomalies in the African troposphere follow a different regime. Fires are much more frequent and are responsible for a large proportion of the CO anomalies, even in the lower layers of the troposphere. In the DJFM, fires occur in the tropical northern side of the continent, so the Gulf of Guinea is mainly affected. In addition, this region is a major emitter of anthropogenic CO and the mixing ratios of the anomalies are very high during this season. During this season in Southern Africa, CO anomalies are more intense in the UT than in the MT, highlighting the importance of the upper branch circulation of the Hadley cell for the transport of pollutant in this region. In JJASO, it is mainly the southern part that is affected by fires. In fact, fire emissions are responsible for almost all the CO anomalies detected in this region/season. The Middle East is relatively unaffected by fires in LT and MT and its anthropogenic pollution is essentially local. However, the upper part of the Northern African and Middle Eastern troposphere can be strongly polluted by African fires during DJFM.

To summarise, the CO anomalies observed throughout the troposphere over Africa are deeply influenced by the intensity of the emissions (both atnthropogenic and BB) and the active convective activity from the Tropics. In the LT, the anomalies are the most intense and are linked with local emissions. Higher up, the anomalies are caused by emissions from further away and are deeply influenced by the ITCZ shift and the variation of wet/dry season.

O_3 mixing ratios in the CO anomalies vary considerably from region to region. For example, in the lower troposphere over the Middle East, where the plumes are mainly due to local anthropogenic emissions, O_3 levels are below the 25th percentile. In the Gulf of Guinea and South Africa we observe O_3 levels above background (even above 75th percentile for South Africa) in the fire plumes during their respective dry seasons, and lower or near background levels during their wet seasons. The signal described above is further enhanced in the middle troposphere and O_3 values in the CO anomalies can reach the 95th percentile during the respective dry seasons of the Gulf of Guinea and South Africa. The fact that these high values are mainly observed in the mid-troposphere and not in the LT, where emissions occur, confirms that a minimum age of air masses must be respected to allow time for photochemistry to take place. For these two regions, the signal in the UT is similar, although attenuated (O_3 levels no longer reach the 75th percentile in the Gulf of Guinea, but remain high in South Africa).

Our study is based on extreme CO mixing ratios, which we have defined as observations above the regional and seasonal the 95th percentile. In order to ensure the robustness of the results with respect to this parameter, we performed a sensitivity test to check whether any major changes in the features could be observed with a thresholds defined as the 75th or 99th percentile. Overall, the same characteristics were observed with just a few differences. In the Northern Hemisphere, increasing the threshold causes a slight increase in the proportion of fire-related plumes (diagnosed as BB or Mix), which is not surprising as we have seen that these plumes are the most intense most of the time. In addition, we observed that our anthropogenic plumes in the UT having an East Asian origin are proportionally more numerous at the highest percentile. In the UT The African plumes appear to be even less sensitive to a change in the threshold.

This study provides useful diagnostics to characterise the high levels of CO in the troposphere at northern mid-latitudes and over India, Africa and Middle-East. The characteristics of those plumes of CO anomalies are described for the seasons of (i)

https://doi.org/10.5194/egusphere-2023-2949
Preprint. Discussion started: 15 January 2024

the most intense fire activity and (ii) the maximum of anthropogenic emissions with respect to the effect of those emissions on the CO distributions in the troposphere. A start has been made on characterising the O_3 levels within our CO anomalies.

This study provides useful diagnostics to characterise the high levels of CO in the troposphere at northern mid-latitudes and over India, Africa and Middle-East. The characteristics of those plumes of CO anomalies are described for the seasons of (i) the most intense fire activity and (ii) the maximum of anthropogenic emissions with respect to the effect of those emissions on the CO distributions in the troposphere. Thanks to the simultaneously recorded O_3 mixing ratios, the diagnostics provided by this study include a first assessment of the O_3 levels within the extreme CO anomalies. To go further in the understanding of the chemical characterisation of these CO anomalies and their impact on the atmospheric composition (not only O_3) at global scale, we obviously need additional data and designed chemistry-transport-model outputs.

Data availability. The IAGOS data (IAGOS, 2022) are available at the IAGOS data portal (https://doi.org/10.25326/20) and more precisely, the time series data are found at https://doi.org/10.25326/06 (Boulanger et al., 2018).

https://doi.org/10.5194/egusphere-2023-2949
Preprint. Discussion started: 15 January 2024

Figure A1. Data availability (number of measured points per regions)

https://doi.org/10.5194/egusphere-2023-2949
Preprint. Discussion started: 15 January 2024

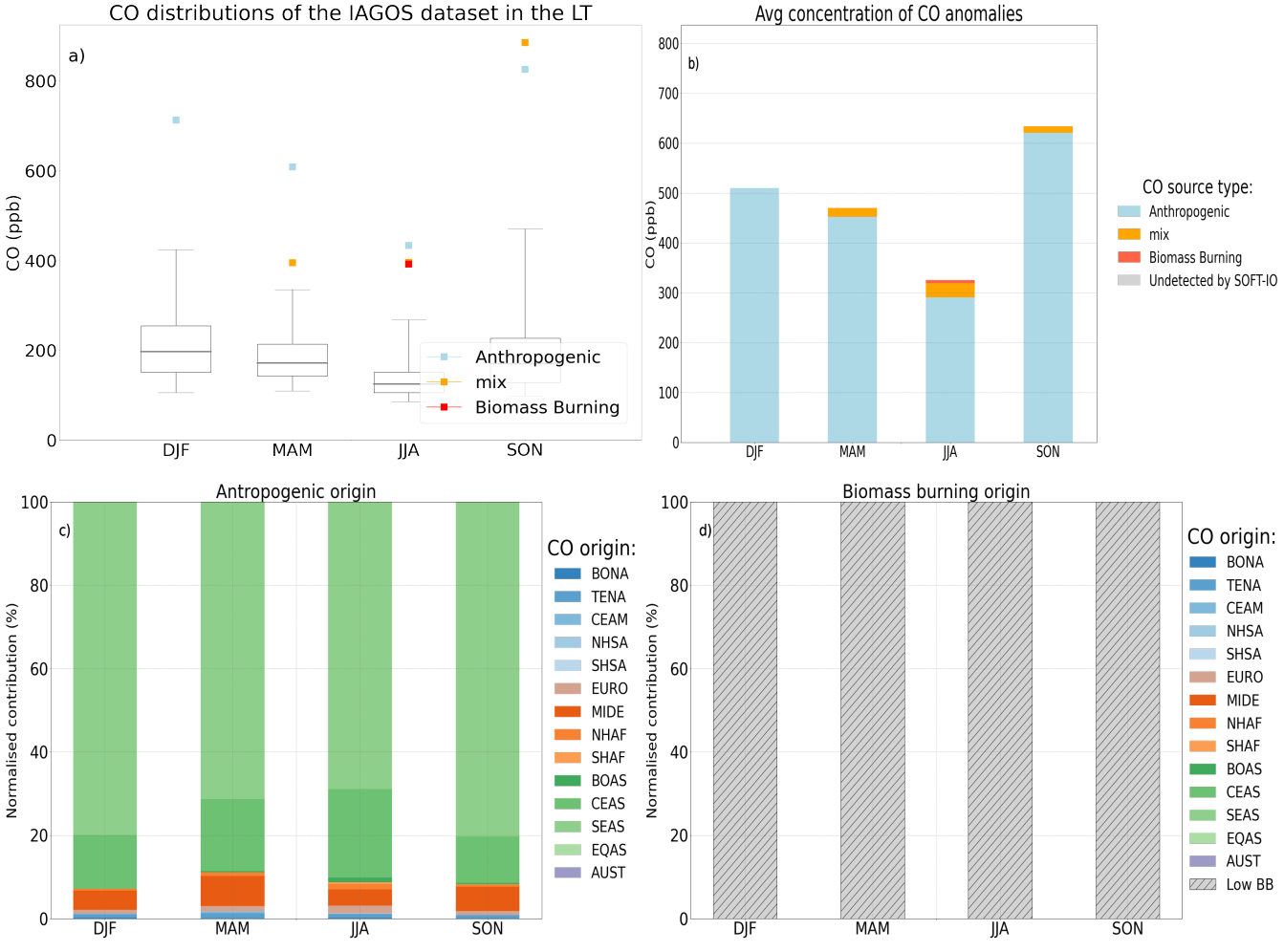

Figure D1. Same as Fig.3 but only for the Indian region during the four seasons for the LT (below 2000m). At this altitude no anomalies are undetected by SOFT-IO (in grey on panel b).

https://doi.org/10.5194/egusphere-2023-2949
Preprint. Discussion started: 15 January 2024

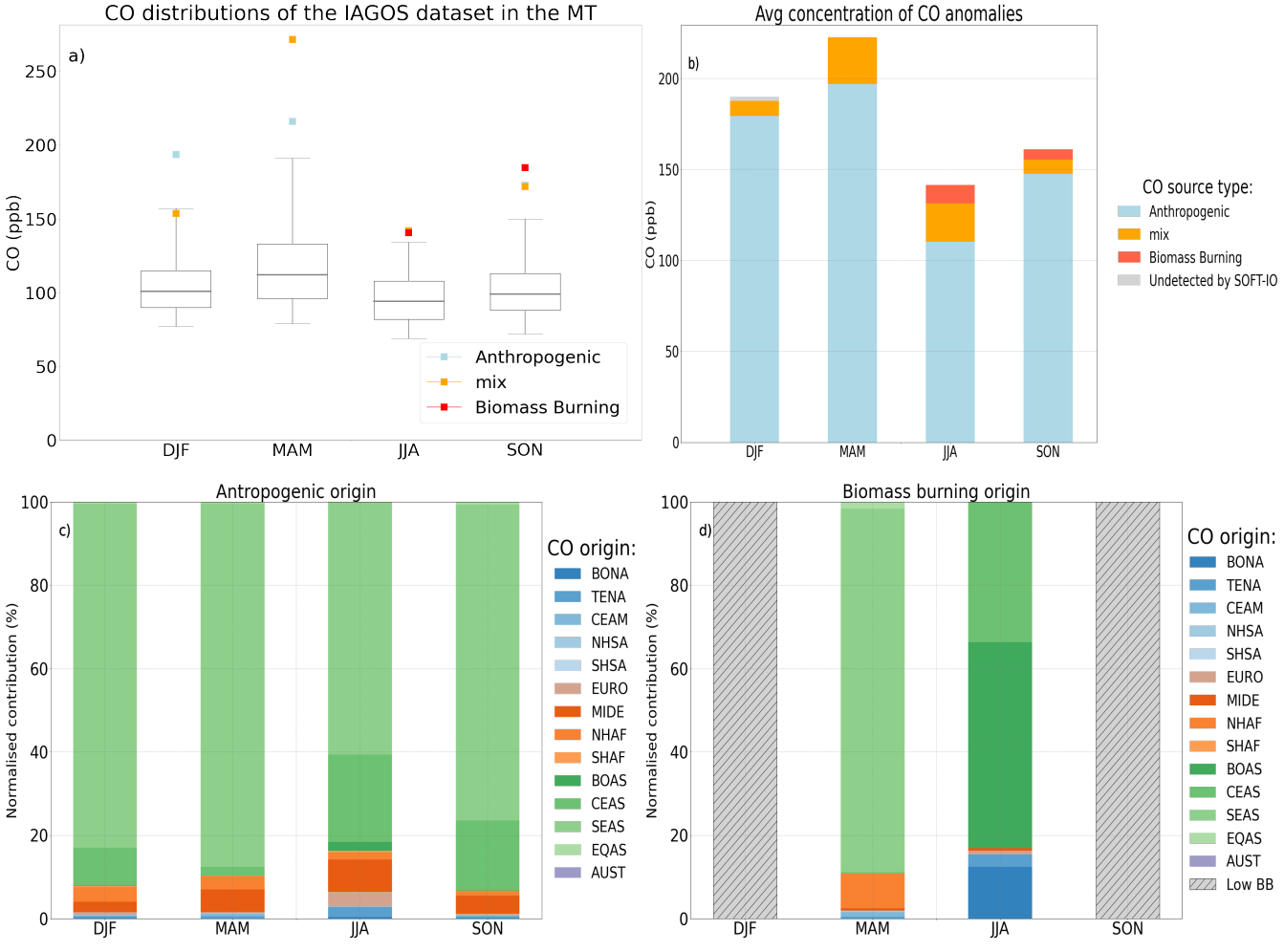

Figure E1. Same as Fig.3 but only for the Indian region during the four seasons for the MT (between 2000m and 8000m). At this altitude 2 anomalies are undetected by SOFT-IO (in grey on panel b).

Author contributions. TL,BS, BJ VM and VT designed the study. The IAGOS and SOFT-IO data were provided by BS, PW, YB, RB, DB, HC, JMC, PN and VT. The paper was written by TL and reviewed by VT, and edited and approved by all the authors.

Competing interests. The authors declare that they have no conflict of interest.

https://doi.org/10.5194/egusphere-2023-2949
Preprint. Discussion started: 15 January 2024

Acknowledgements. We acknowledge the strong support of the European Commission, Airbus and the airlines (Deutsche Lufthansa, Air France, Austrian, Air Namimbia, Cathay Pacific, Iberia, China Airlines, Hawaiian Airlines, and Air Canada so far) that have carried the MOZAIC or IAGOS equipment and performed the maintenance since 1994. IAGOS has been funded by the European Union projects IAGOS–DS and IAGOS–ERI. Additionally, IAGOS has been funded by INSU-CNRS (France), Météo-France, Université Paul Sabatier (Toulouse, France) and Research Center Jülich (FZJ, Jülich, Germany). The IAGOS database is supported in France by AERIS (https://www.aeris-data.fr)

https://doi.org/10.5194/egusphere-2023-2949
Preprint. Discussion started: 15 January 2024

References

Andreae, M. O., Artaxo, P., Fischer, H., Freitas, S., Grégoire, J.-M., Hansel, A., Hoor, P., Kormann, R., Krejci, R., Lange, L., et al.: Transport of biomass burning smoke to the upper troposphere by deep convection in the equatorial region, Geophysical Research Letters, 28, 951–954, 2001.

Ashmore, M.: Assessing the future global impacts of ozone on vegetation, Plant, Cell & Environment, 28, 949–964, 2005.

Barret, B., Ricaud, P., Mari, C., Attié, J.-L., Bousserez, N., Josse, B., Le Flochmoën, E., Livesey, N., Massart, S., Peuch, V.-H., et al.: Transport pathways of CO in the African upper troposphere during the monsoon season: a study based upon the assimilation of spaceborne observations, Atmospheric Chemistry and Physics, 8, 3231–3246, 2008.

Barret, B., Sauvage, B., Bennouna, Y., and Le Flochmoen, E.: Upper-tropospheric CO and O 3 budget during the Asian summer monsoon, Atmospheric Chemistry and Physics, 16, 9129–9147, 2016.

Bergman, J. W., Fierli, F., Jensen, E. J., Honomichl, S., and Pan, L. L.: Boundary layer sources for the Asian anticyclone: Regional contributions to a vertical conduit, Journal of Geophysical Research: Atmospheres, 118, 2560–2575, 2013.

Blot, R., Nedelec, P., Boulanger, D., Wolff, P., Sauvage, B., Cousin, J.-M., Athier, G., Zahn, A., Obersteiner, F., Scharffe, D., et al.: Internal consistency of the IAGOS ozone and carbon monoxide measurements for the last 25 years, Atmospheric Measurement Techniques, 14, 3935–3951, 2021.

Brenninkmeijer, C., Crutzen, P., Fischer, H., Güsten, H., Hans, W., Heinrich, G., Heintzenberg, J., Hermann, M., Immelmann, T., Kersting, D., et al.: CARIBIC—Civil aircraft for global measurement of trace gases and aerosols in the tropopause region, Journal of Atmospheric and Oceanic Technology, 16, 1373–1383, 1999.

Chen, T.-M., Kuschner, W. G., Gokhale, J., and Shofer, S.: Outdoor air pollution: ozone health effects, The American journal of the medical sciences, 333, 244–248, 2007.

Cohen, Y., Petetin, H., Thouret, V., Marécal, V., Josse, B., Clark, H., Sauvage, B., Fontaine, A., Athier, G., Blot, R., et al.: Climatology and long-term evolution of ozone and carbon monoxide in the upper troposphere–lower stratosphere (UTLS) at northern midlatitudes, as seen by IAGOS from 1995 to 2013, Atmospheric Chemistry and Physics, 18, 5415–5453, 2018.

Cussac, M., Marécal, V., Thouret, V., Josse, B., and Sauvage, B.: The impact of biomass burning on upper tropospheric carbon monoxide: a study using MOCAGE global model and IAGOS airborne data, Atmospheric Chemistry and Physics, 20, 9393–9417, 2020.

Damoah, R., Spichtinger, N., Servranckx, R., Fromm, M., Eloranta, E., Razenkov, I., James, P., Shulski, M., Forster, C., and Stohl, A.: A case study of pyro-convection using transport model and remote sensing data, Atmospheric Chemistry and Physics, 6, 173–185, 2006.

Davison, A. and Barnes, J.: Effects of ozone on wild plants, The New Phytologist, 139, 135–151, 1998.

Fadnavis, S., Buchunde, P., Ghude, S. D., Kulkarni, S., and Beig, G.: Evidence of seasonal enhancement of CO in the upper troposphere over India, International journal of remote sensing, 32, 7441–7452, 2011.

Fuhrer, J., Skärby, L., and Ashmore, M. R.: Critical levels for ozone effects on vegetation in Europe, Environmental pollution, 97, 91–106, 1997.

Galanter, M., Levy, H., and Carmichael, G. R.: Impacts of biomass burning on tropospheric CO, NO x, and O3, Journal of Geophysical Research: Atmospheres, 105, 6633–6653, 2000.

Giglio, L., Randerson, J. T., and Van Der Werf, G. R.: Analysis of daily, monthly, and annual burned area using the fourth-generation global fire emissions database (GFED4), Journal of Geophysical Research: Biogeosciences, 118, 317–328, 2013.

https://doi.org/10.5194/egusphere-2023-2949
Preprint. Discussion started: 15 January 2024

Huang, L., Fu, R., Jiang, J., Wright, J., and Luo, M.: Geographic and seasonal distributions of CO transport pathways and their roles in determining CO centers in the upper troposphere, Atmospheric Chemistry and Physics, 12, 4683–4698, 2012.

IPCC: The physical science basis: Working group I contribution to the fifth assessment report of the Intergovernmental Panel on Climate Change, Stocker, T.F., D. Qin, G.-K. Plattner, M. Tignor, S.K. Allen, J. Boschung, A. Nauels, Y. Xia, V. Bex and P.M. Midgley, p. 1535, 2013.

Kaiser, J., Heil, A., Andreae, M., Benedetti, A., Chubarova, N., Jones, L., Morcrette, J.-J., Razinger, M., Schultz, M., Suttie, M., et al.: Biomass burning emissions estimated with a global fire assimilation system based on observed fire radiative power, Biogeosciences, 9, 527–554, 2012.

Labonne, M., Bréon, F.-M., and Chevallier, F.: Injection height of biomass burning aerosols as seen from a spaceborne lidar, Geophysical Research Letters, 34, 2007.

Lannuque, V., Sauvage, B., Barret, B., Clark, H., Athier, G., Boulanger, D., Cammas, J.-P., Cousin, J.-M., Fontaine, A., Le Flochmoën, E., et al.: Origins and characterization of CO and O 3 in the African upper troposphere, Atmospheric chemistry and physics, 21, 14 535–14 555, 2021.

Lawrence, M. G.: Export of air pollution from southern Asia and its large-scale effects, Air Pollution, pp. 131–172, 2004.

Lelieveld, J., Gromov, S., Pozzer, A., and Taraborrelli, D.: Global tropospheric hydroxyl distribution, budget and reactivity, Atmospheric Chemistry and Physics, 16, 12 477–12 493, 2016.

Liang, Q., Jaeglé, L., Jaffe, D. A., Weiss-Penzias, P., Heckman, A., and Snow, J. A.: Long-range transport of Asian pollution to the northeast Pacific: Seasonal variations and transport pathways of carbon monoxide, Journal of Geophysical Research: Atmospheres, 109, 2004.

Liu, H., Liu, S., Xue, B., Lv, Z., Meng, Z., Yang, X., Xue, T., Yu, Q., and He, K.: Ground-level ozone pollution and its health impacts in China, Atmospheric environment, 173, 223–230, 2018.

Marenco, A., Thouret, V., Nédélec, P., Smit, H., Helten, M., Kley, D., Karcher, F., Simon, P., Law, K., Pyle, J., et al.: Measurement of ozone and water vapor by Airbus in-service aircraft: The MOZAIC airborne program, An overview, Journal of Geophysical Research: Atmospheres, 103, 25 631–25 642, 1998.

Mauzerall, D. L., Logan, J. A., Jacob, D. J., Anderson, B. E., Blake, D. R., Bradshaw, J. D., Heikes, B., Sachse, G. W., Singh, H., and Talbot, B.: Photochemistry in biomass burning plumes and implications for tropospheric ozone over the tropical South Atlantic, Journal of Geophysical Research: Atmospheres, 103, 8401–8423, 1998.

McDuffie, E. E., Smith, S. J., O'Rourke, P., Tibrewal, K., Venkataraman, C., Marais, E. A., Zheng, B., Crippa, M., Brauer, M., and Martin, R. V.: A global anthropogenic emission inventory of atmospheric pollutants from sector-and fuel-specific sources (1970–2017): an application of the Community Emissions Data System (CEDS), Earth System Science Data, 12, 3413–3442, 2020.

Nedelec, P., Thouret, V., Brioude, J., Sauvage, B., Cammas, J.-P., and Stohl, A.: Extreme CO concentrations in the upper troposphere over northeast Asia in June 2003 from the in situ MOZAIC aircraft data, Geophysical Research Letters, 32, 2005.

Nédélec, P., Blot, R., Boulanger, D., Athier, G., Cousin, J.-M., Gautron, B., Petzold, A., Volz-Thomas, A., and Thouret, V.: Instrumentation on commercial aircraft for monitoring the atmospheric composition on a global scale: the IAGOS system, technical overview of ozone and carbon monoxide measurements, Tellus B: Chemical and Physical Meteorology, 67, 27 791, 2015.

Nicholson, S. E.: The ITCZ and the seasonal cycle over equatorial Africa, Bulletin of the American Meteorological Society, 99, 337–348, 2018.

Owen, R., Cooper, O., Stohl, A., and Honrath, R.: An analysis of the mechanisms of North American pollutant transport to the central North Atlantic lower free troposphere, Journal of Geophysical Research: Atmospheres, 111, 2006.

https://doi.org/10.5194/egusphere-2023-2949
Preprint. Discussion started: 15 January 2024

Pan, L. L., Honomichl, S. B., Kinnison, D. E., Abalos, M., Randel, W. J., Bergman, J. W., and Bian, J.: Transport of chemical tracers from the boundary layer to stratosphere associated with the dynamics of the Asian summer monsoon, Journal of Geophysical Research: Atmospheres, 121, 14–159, 2016.

Park, M., Randel, W. J., Gettelman, A., Massie, S. T., and Jiang, J. H.: Transport above the Asian summer monsoon anticyclone inferred from Aura Microwave Limb Sounder tracers, Journal of Geophysical Research: Atmospheres, 112, 2007.

Park, M., Randel, W. J., Emmons, L. K., Bernath, P. F., Walker, K. A., and Boone, C. D.: Chemical isolation in the Asian monsoon anticyclone observed in Atmospheric Chemistry Experiment (ACE-FTS) data, Atmospheric Chemistry and Physics, 8, 757–764, 2008.

Paugam, R., Wooster, M., Atherton, J., Freitas, S., Schultz, M., and Kaiser, J.: Development and optimization of a wildfire plume rise model based on remote sensing data inputs–Part 2, Atmospheric Chemistry and Physics Discussions, 15, 9815–9895, 2015.

Petetin, H., Thouret, V., Fontaine, A., Sauvage, B., Athier, G.and Blot, R., Boulanger, D., Cousin, J.-M., and Nédélec, P.: Representativeness of the IAGOS airborne measurements in the lower troposphere, Atmospheric Chemistry and Physics, 16, 2016.

Petetin, H., Jeoffrion, M., Sauvage, B., Athier, G., Blot, R., Boulanger, D., Clark, H., Cousin, J.-M., Gheusi, F., Nedelec, P., et al.: Representativeness of the IAGOS airborne measurements in the lower troposphere, Elementa: Science of the Anthropocene, 6, 2018a.

Petetin, H., Sauvage, B., Parrington, M., Clark, H., Fontaine, A., Athier, G., Blot, R., Boulanger, D., Cousin, J.-M., Nédélec, P., et al.: The role of biomass burning as derived from the tropospheric CO vertical profiles measured by IAGOS aircraft in 2002–2017, Atmospheric Chemistry and Physics, 18, 17 277–17 306, 2018b.

Petzold, A., Thouret, V., Gerbig, C., Zahn, A., Brenninkmeijer, C. A., Gallagher, M., Hermann, M., Pontaud, M., Ziereis, H., Boulanger, D., et al.: Global-scale atmosphere monitoring by in-service aircraft–current achievements and future prospects of the European Research Infrastructure IAGOS, Tellus B: Chemical and Physical Meteorology, 67, 28 452, 2015.

Pochanart, P., Wild, O., and Akimoto, H.: Air pollution import to and export from East Asia, Air pollution: Intercontinental transport of air pollution, pp. 99–130, 2004.

Rémy, S., Veira, A., Paugam, R., Sofiev, M., Kaiser, J. W., Marenco, F., Burton, S. P., Benedetti, A., Engelen, R. J., Ferrare, R., et al.: Two global data sets of daily fire emission injection heights since 2003, Atmospheric Chemistry and Physics, 17, 2921–2942, 2017.

Ricaud, P., Sič, B., El Amraoui, L., Attié, J.-L., Zbinden, R., Huszar, P., Szopa, S., Parmentier, J., Jaidan, N., Michou, M., et al.: Impact of the Asian monsoon anticyclone on the variability of mid-to-upper tropospheric methane above the Mediterranean Basin, Atmospheric Chemistry and Physics, 14, 11 427–11 446, 2014.

Riese, M., Ploeger, F., Rap, A., Vogel, B., Konopka, P., Dameris, M., and Forster, P.: Impact of uncertainties in atmospheric mixing on simulated UTLS composition and related radiative effects, Journal of Geophysical Research: Atmospheres, 117, 2012.

Sauvage, B., Thouret, V., Cammas, J.-P., Gheusi, F., Athier, G., and Nédélec, P.: Tropospheric ozone over Equatorial Africa: regional aspects from the MOZAIC data, Atmospheric Chemistry and Physics, 5, 311–335, 2005.

Sauvage, B., Fontaine, A., Eckhardt, S., Auby, A., Boulanger, D., Petetin, H., Paugam, R., Athier, G., Cousin, J.-M., Darras, S., et al.: Source attribution using FLEXPART and carbon monoxide emission inventories: SOFT-IO version 1.0, Atmospheric Chemistry and Physics, 17, 15 271–15 292, 2017.

Seinfeld, J. and Pandis, S.: Atmospheric chemistry and physics. 1997, New York, 2008.

Smoydzin, L. and Hoor, P.: Contribution of Asian emissions to upper tropospheric CO over the remote Pacific, Atmospheric Chemistry and Physics, 22, 7193–7206, 2022.

Stohl, A., Forster, C., Frank, A., Seibert, P., and Wotawa, G.: The Lagrangian particle dispersion model FLEXPART version 6.2, Atmospheric Chemistry and Physics, 5, 2461–2474, 2005.

https://doi.org/10.5194/egusphere-2023-2949
Preprint. Discussion started: 15 January 2024

Thouret, V., Marenco, A., Logan, J. A., Nédélec, P., and Grouhel, C.: Comparisons of ozone measurements from the MOZAIC airborne program and the ozone sounding network at eight locations, Journal of Geophysical Research: Atmospheres, 103, 25 695–25 720, 1998.

Thouret, V., Cammas, J.-P., Sauvage, B., Athier, G., Zbinden, R., Nédélec, P., Simon, P., and Karcher, F.: Tropopause referenced ozone climatology and inter-annual variability (1994–2003) from the MOZAIC programme, Atmospheric Chemistry and Physics, 6, 1033–1051, 2006.

Thouret, V., Clark, H., Petzold, A., Nédélec, P., and Zahn, A.: IAGOS: Monitoring Atmospheric Composition for Air Quality and Climate by Passenger Aircraft, Handbook of Air Quality and Climate Change, 18, 17 277–17 306, 2022.

Tsivlidou, M., Sauvage, B., Barret, B., Wolff, P., Clark, H., Bennouna, Y., Blot, R., Boulanger, D., Nédélec, P., Le Flochmoën, E., et al.: Tropical tropospheric ozone and carbon monoxide distributions: characteristics, origins and control factors, as seen by IAGOS and IASI, Atmospheric Chemistry and Physics Discussions, pp. 1–50, 2022.

Val Martin, M., Logan, J., Kahn, R., Leung, F.-Y., Nelson, D., and Diner, D.: Smoke injection heights from fires in North America: analysis of 5 years of satellite observations, Atmospheric Chemistry and Physics, 10, 1491–1510, 2010.

Xia, Y., Huang, Y., and Hu, Y.: On the climate impacts of upper tropospheric and lower stratospheric ozone, Journal of Geophysical Research: Atmospheres, 123, 730–739, 2018.

https://doi.org/10.5194/egusphere-2023-2949
Preprint. Discussion started: 15 January 2024

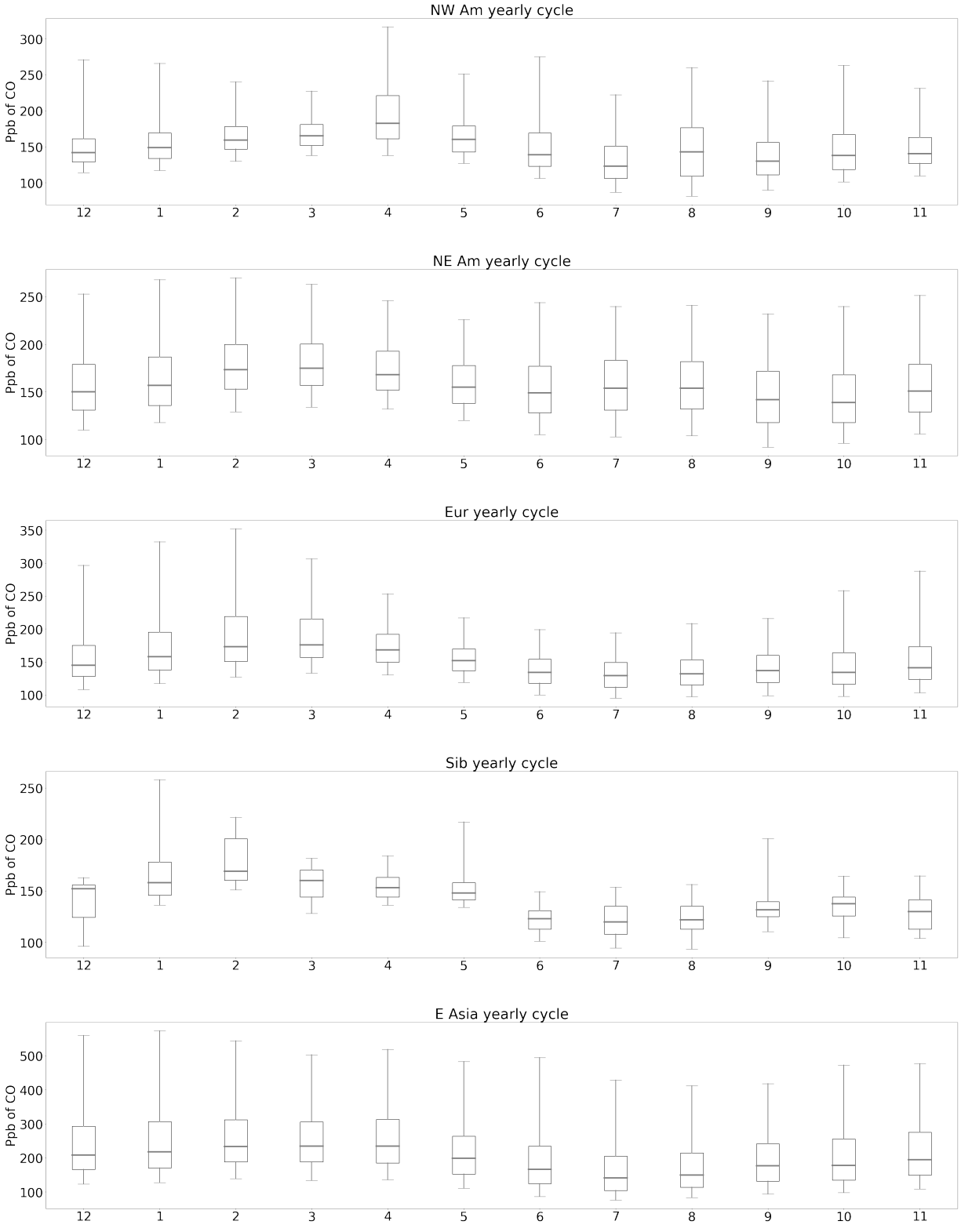

Figure B1. CO yearly cycle

https://doi.org/10.5194/egusphere-2023-2949
Preprint. Discussion started: 15 January 2024

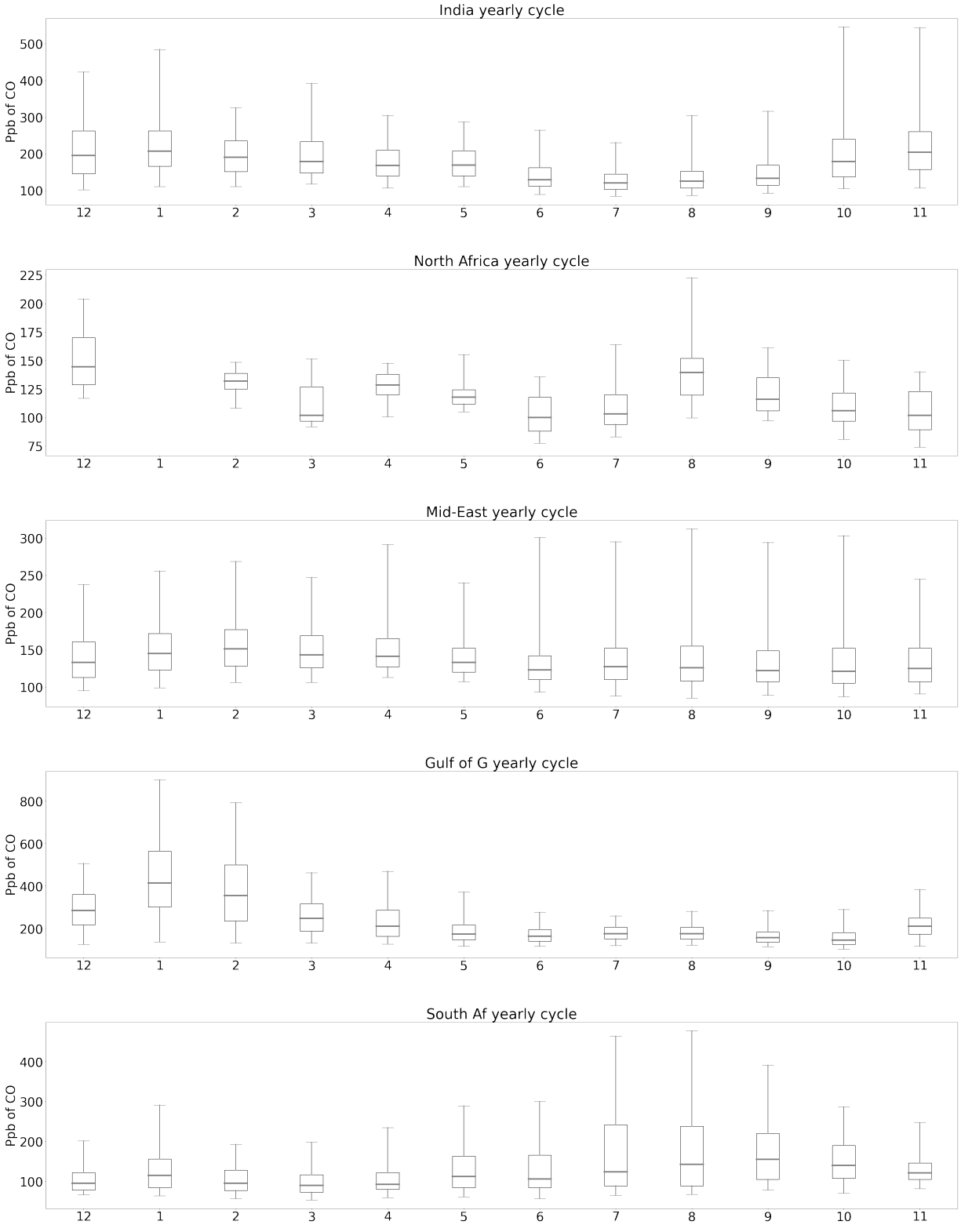

Figure C1. CO yearly cycle